10.21611/qirt.2016.d

UNIVERSITY OF NAPLES *FEDERICO II*
Department of Industrial Engineering – Aerospace Division

1224

An Excursus of Some Research Performed with Infrared Thermography at Federico II

Giovanni Maria Carlomagno,
Università di Napoli *Federico II* – DII
carmagno@unina.it

QIRT 2016 *Conference*
July 4/8, 2016
Gdańsk, Poland

10.21611/qirt.2016.d

SCOPE OF THE PRESENTATION

This presentation reviews some of the experimental and theoretical work carried out, over the past several years, by the speaker and his research team, while applying ***infrared thermography*** to ***thermo-fluid-dynamics*** and ***NDT***.
Most of the work was performed at **University of Naples *Federico II*** and:

- **Centre d'études aérodynamiques et thermiques** (CEAT), Poitiers, France
- **Università di Pisa**, Pisa, Italy
- **University of Tokyo**, Tokyo, Japan
- **Italian Centre for Aerospace Research** (CIRA), Capua, Italy
- **Centro Spazio** (Space Centre), Pisa, Italy
- **Politecnico di Torino**, Torino, Italy
- **Delft Technical University**, Delft, The Netherlands (prof. Scarano group)
- **Universidad Carlos III de Madrid**, Madrid, Spain

The research team involved in the present work is composed by:

- ***Tommaso Astarita***
- ***Piergiorgio Berardi***
- ***Gennaro Cardone***
- ***Giovanni Maria Carlomagno***
- ***Stefano Discetti***
- ***Luigi de Luca***
- ***Carlo Salvatore Greco***
- ***Andrea Ianiro***
- ***Michele Imbriale***
- ***Carosena Meola***
- ***Several Master and PhD students***
  (***who, actually, performed most of the experiments***)

10.21611/qirt.2016.d

STARTING

At the beginning of the 70ties, our research group started with non-destructive testing.

The isothermal line in a steel slab having a cavity, initially at ambient temperature, suddendly exposed to steam on one side and viewed from the other one.

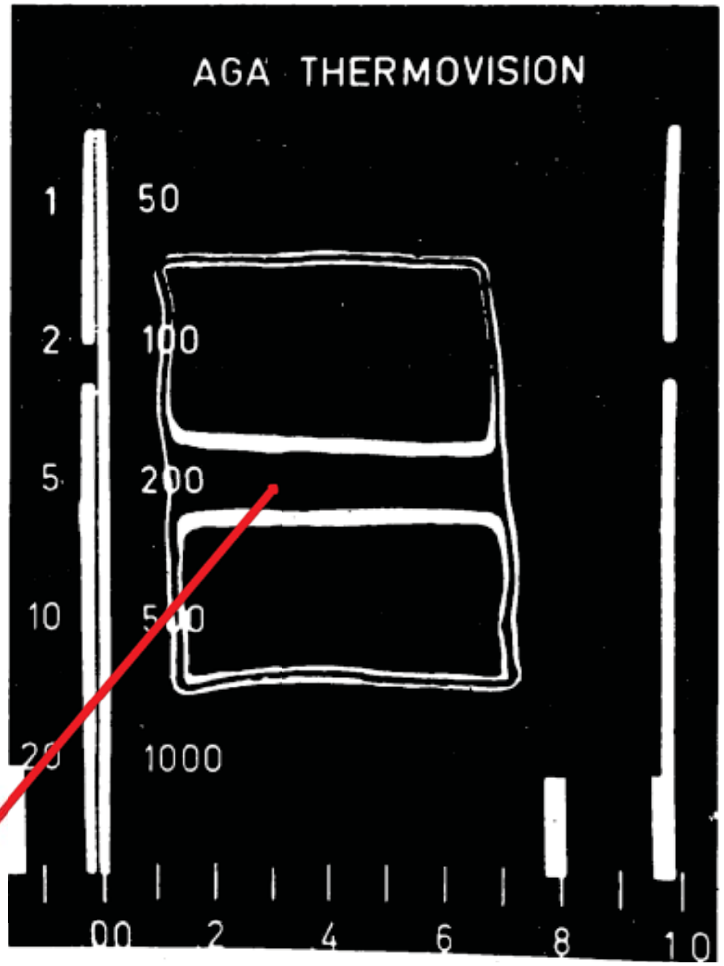

CARLOMAGNO GM and BERARDI PG, Unsteady Thermotopography of Slabs with Inner Cavities, Atti II Cong. Naz. AIMETA, **IV**, 263-272, Napoli (1974)

10.21611/qirt.2016.d

Unsteady thermotopography in non-destructive testing

Giovanni Maria Carlomagno, Pier Giorgio Berardi

Proc. 3rd Biannual Exchange, St. Louis/USA (**IRIE '76**)
Pages 33-40, ***Research Gate***

The present research was focused on the study of unsteady surface temperature fields to obtain information about the internal physical structure of a thermally loaded system, by discriminating among surface temperature differences and their time evolution;

in other words, the idea was to adopt the time variable in the place of the depth variable (i.e. the coordinate normal to the observed surface) to recover knowledge about the "inside" of the system.

Most probably, this work introduced the lock-in concept.

10.21611/qirt.2016.d

NON-DESTRUCTIVE TESTING (Lockin)

Lockin thermography setup

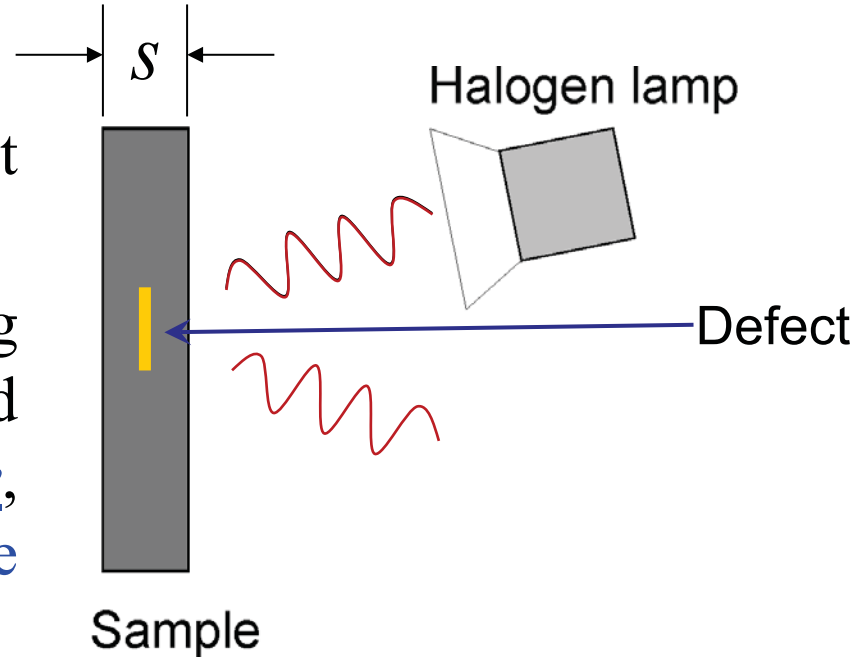

- a ***periodic heat flux*** is incident on the surface of interest
- IR camera monitors the varying sample ***surface temperature*** and local differences of the ***phase***, and/or of the ***amplitude***, response are sought for.

Direct estimation of defect depth

Heat diffusion lenght $\mu = \sqrt{\frac{\alpha}{\pi f}}$

Thermal diffusivity

Heating frequency

For *phase images*, the **thermal penetration depth** is: $p = 1.8\,\mu$

CARLOMAGNO GM and BERARDI PG, Unsteady Thermotopography in Non-Destructive Testing", in Warren C ed., Proc. III Infrared Information Exchange, 33-40, St. Louis (1976)

10.21611/qirt.2016.d

DETECTION OF RESIDUAL CERAMIC
in serpentine cooling passages of turbine blades

Type A blade

Internal core (passages for blade cooling)

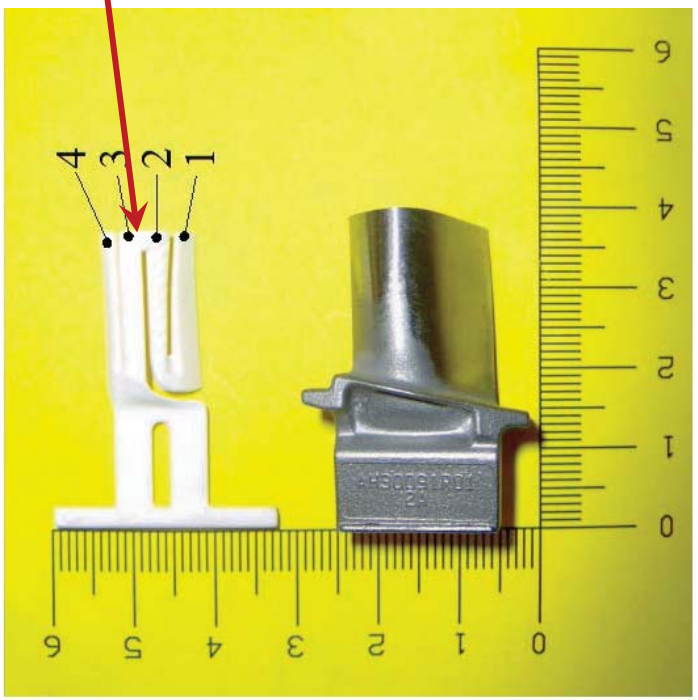

Blade surface viewed by the camera

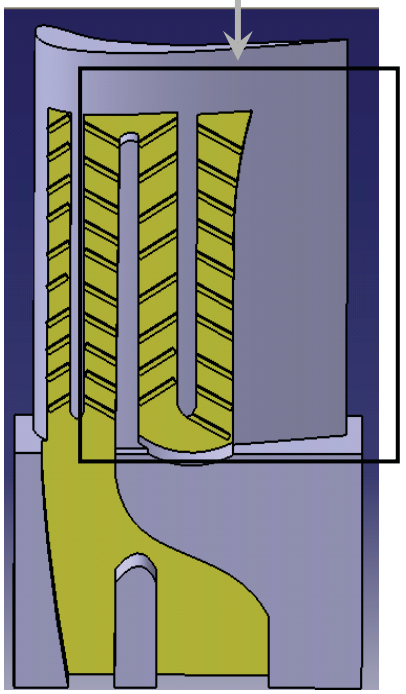

MEOLA C, CARLOMAGNO GM, DI FOGGIA M and NATALE O, Infrared Thermography to Detect Residual Ceramic in Gas Turbine Blades, ***Applied Physics A – Material Science and Processing***, 91, 685-691 (**2008**)

10.21611/qirt.2016.d

Type A blade

Phase images for $f = 0.65$ Hz

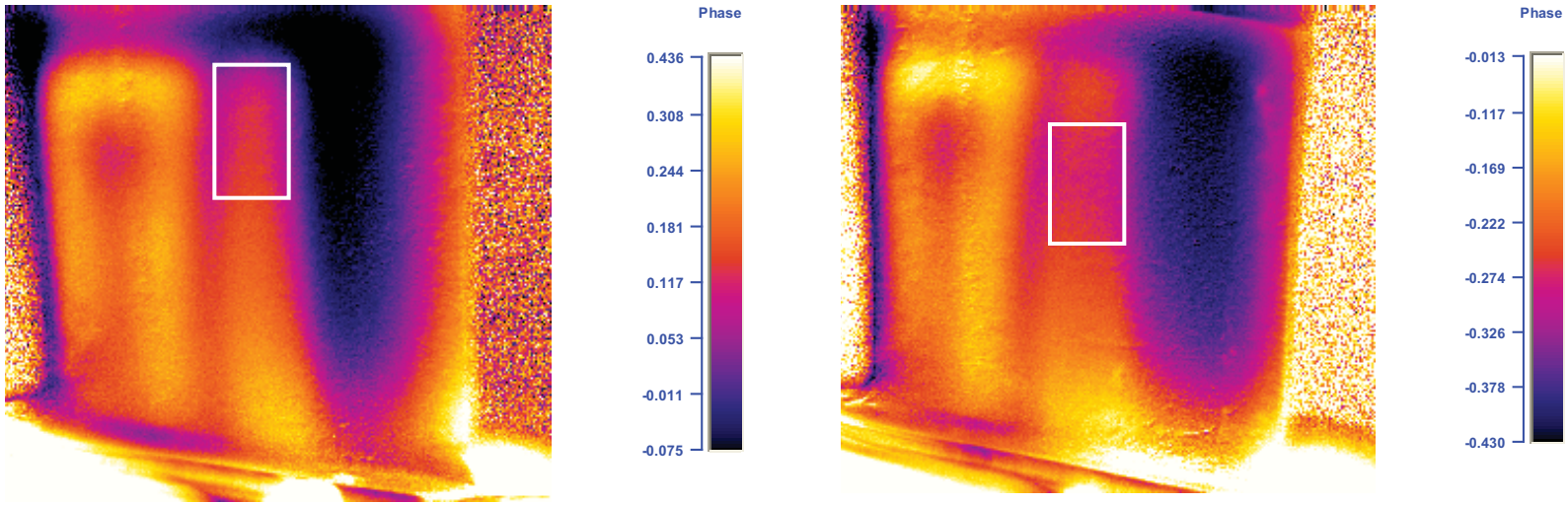

A04 **A13**

The ***phase angle discontinuities*** (inside the white rectangles) in the first channel from the trailing edge (right side) testify the ***presence of residual ceramic***.

10.21611/qirt.2016.d

Type B blade

Serpentine cooling passages

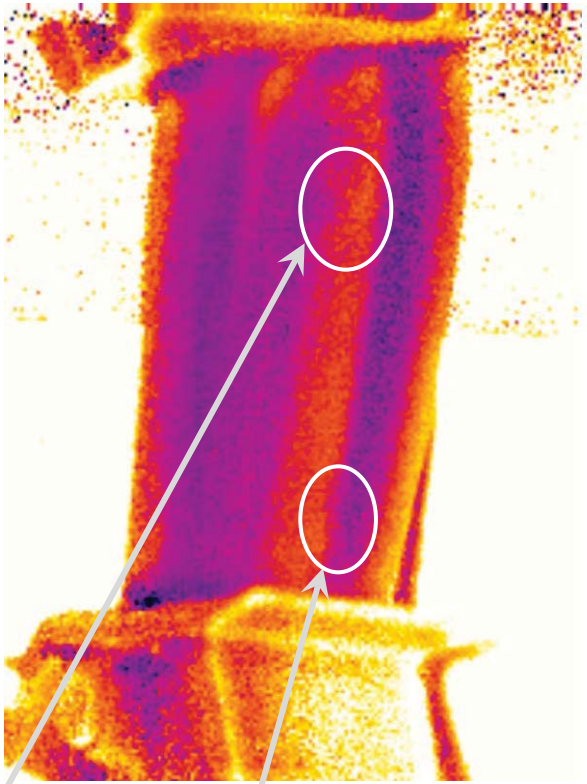

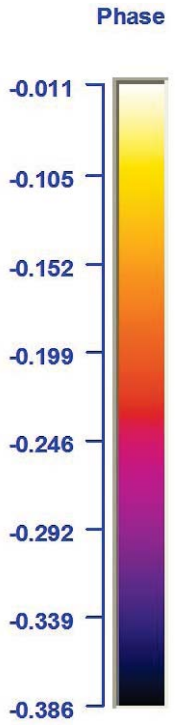

residual ceramic

10.21611/qirt.2016.d

IMPACT EVENTS

(Thermographic on-line monitoring and Non-destructive testing after impact)

MEOLA C and CARLOMAGNO GM, Infrared thermography to impact-driven thermal effects, ***Applied Physics A***, **96**, 759-762 (2009).

MEOLA C and CARLOMAGNO GM, Impact damage in GFRP: new insights with Infrared Thermography, ***Composites Part A***, **41**, 1839-1847 (2010)

10.21611/qirt.2016.d

IMPACT WITH CHARPY PENDULUM

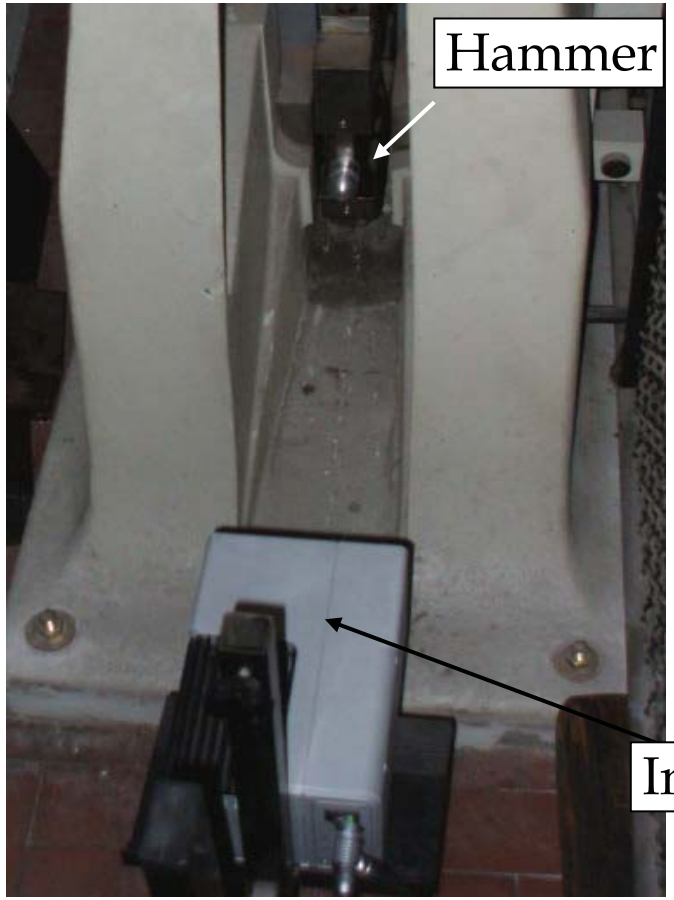

Front view

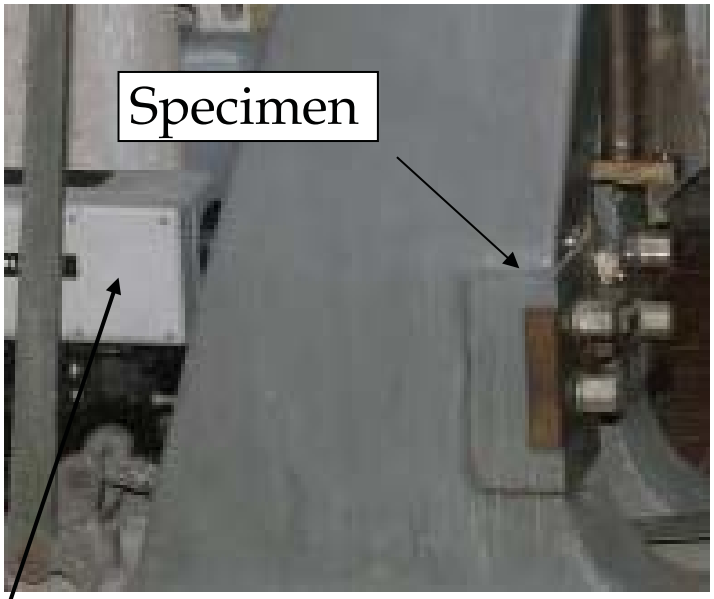

Side view

10.21611/qirt.2016.d

DATA ANALYSIS

The ***first image*** $T(i, j, t=0)$ of the sequence (i.e. the specimen surface at ambient temperature, before the impact) ***is subtracted*** to each subsequent image so as to generate a map of ***temperature difference*** ΔT caused by the impact:

$$\Delta T = T(i,j,t) - T(i,j,0)$$

where: i and j represent lines and columns of the surface temperature matrix, respectively.

Then, a sequence of ***ΔT images*** is created.

Samples of GFRP and Glare® are tested.

10.21611/qirt.2016.d

HIGH SPEED ACQUISITION OF THERMAL IMAGES

GFRP with the SC3000

at 300*Hz* images are composed of 48 lines

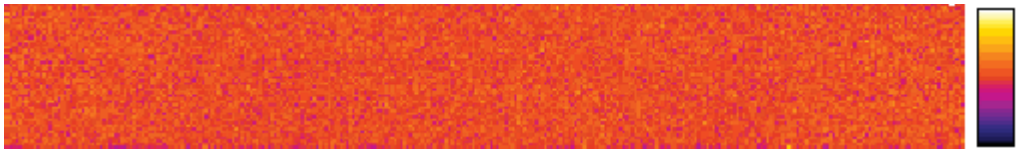

at 900*Hz* images are composed of 16 lines

10.21611/qirt.2016.d

TIME-SEQUENCE PLOT OF ΔT IN A POINT BESIDES THE IMPACT ZONE

GFRP , $E_i = 12J$, SC3000 at 900Hz

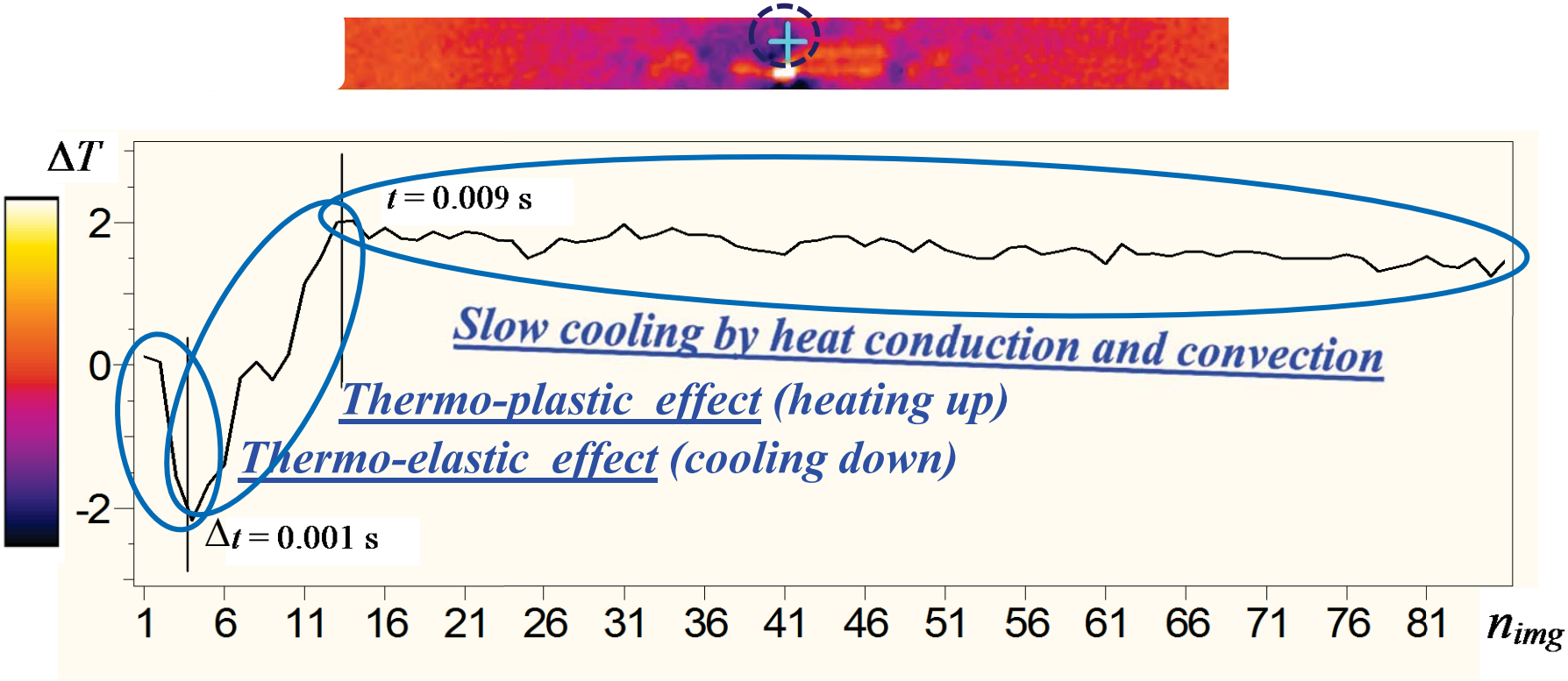

MEOLA C and CARLOMAGNO GM, Infrared thermography to impact-driven thermal effects, ***Applied Physics A***, vol. 96, pp. 759-762 (2009).

10.21611/qirt.2016.d

SEQUENCE OF ΔT IMAGES

GFRP, E_i = 19*J*, taken at 300*Hz* with SC3000

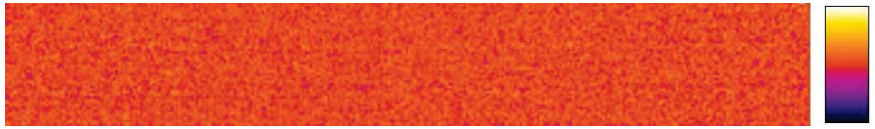

Before impact

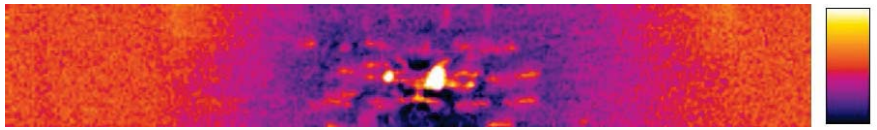

t = 0.0033s

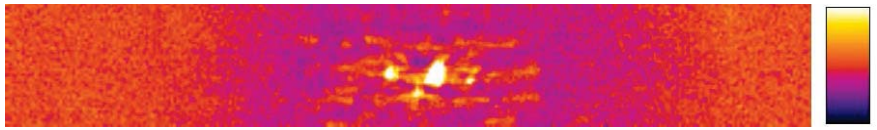

t = 0.01s

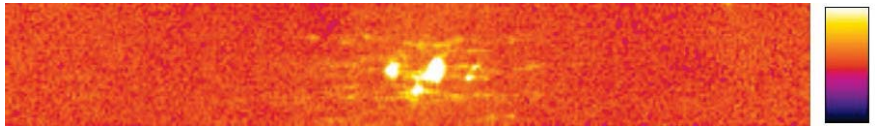

t = 0.02s

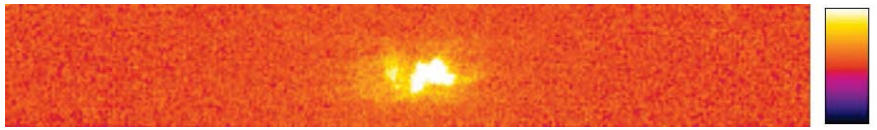

t = 0.40s

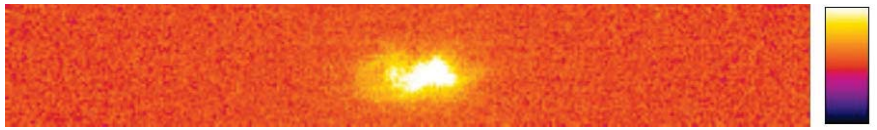

t = 0.90s

10.21611/qirt.2016.d

DAMAGED AREA IN GFRP

Raw *thermal* image taken *during impact*

Lockin *phase* image $f = 0.14Hz$ *after impact* to detect defects

Picture in the *visible* of a translucent GFRP, *after impact*

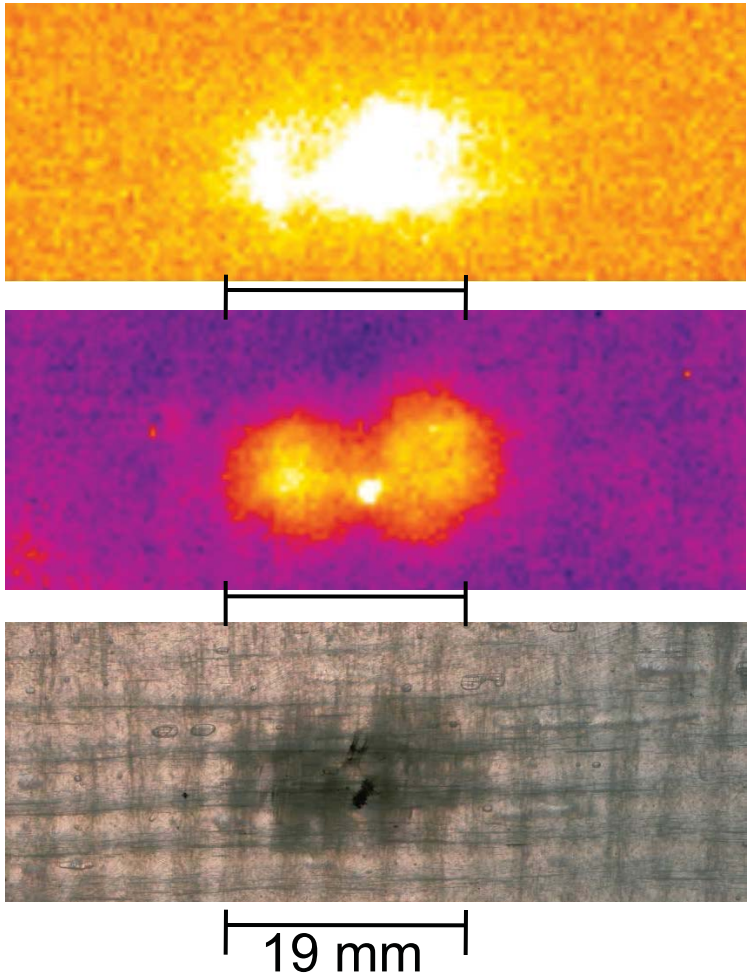

10.21611/qirt.2016.d

SEQUENCE OF ΔT IMAGES OF Glare®

taken with SC3000 at 900*Hz*, specimen impacted at 2.7*J*

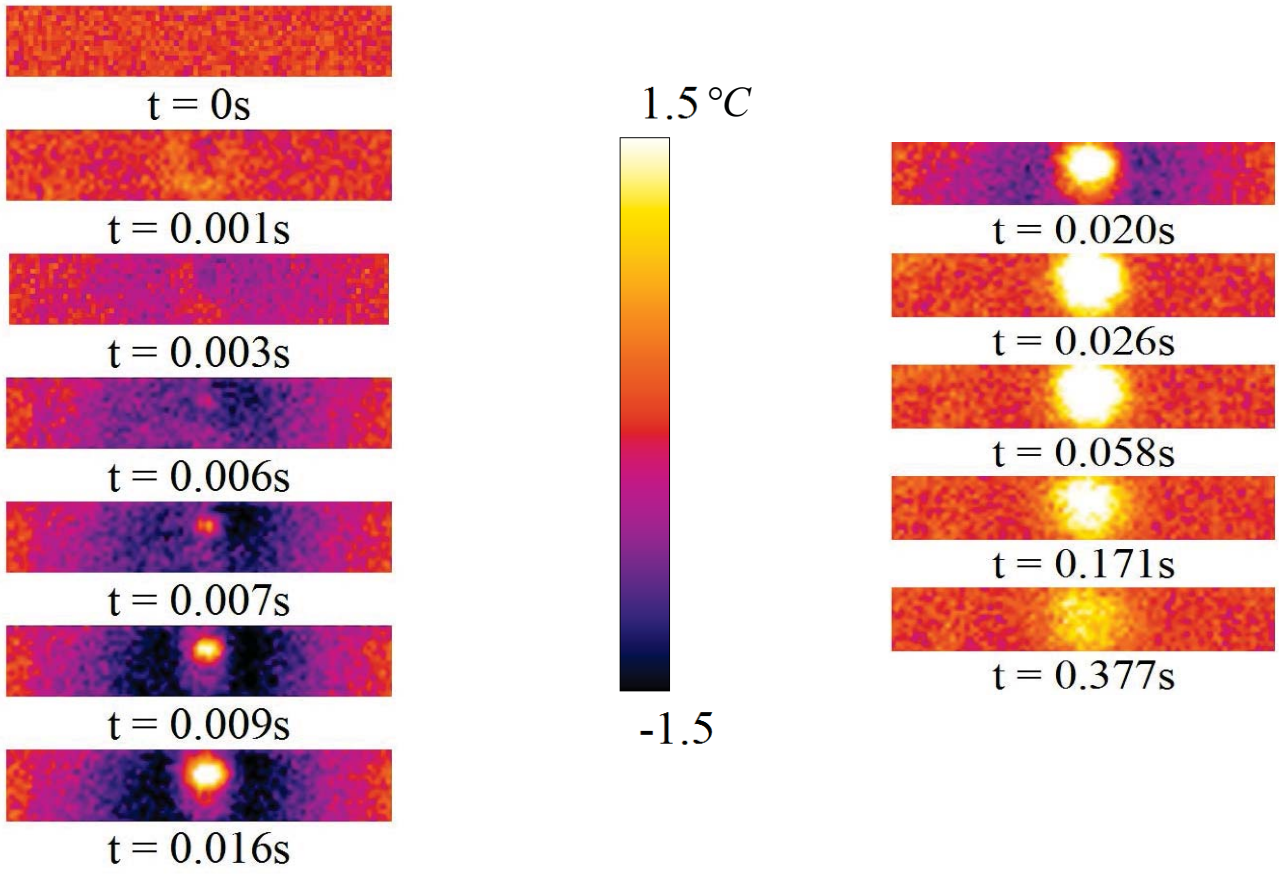

MEOLA C, CARLOMAGNO GM, RICCI F, LOPRESTO V and CAPRINO G, Analisi del Comportamento all'Impatto di Compositi con Termografia all'Infrarosso, Proc. *13° Cong AIPnD,* Rome, (2009), CD-ROM, ISBN 978-88-89758-04-5, www.ndt.net/search/docs.php3?MainSource=-1&id=8199.

10.21611/qirt.2016.d

But, at the time, we had to switch to:

THERMO-FLUID-DYNAMICS

(*that was our most proper business*)

10.21611/qirt.2016.d

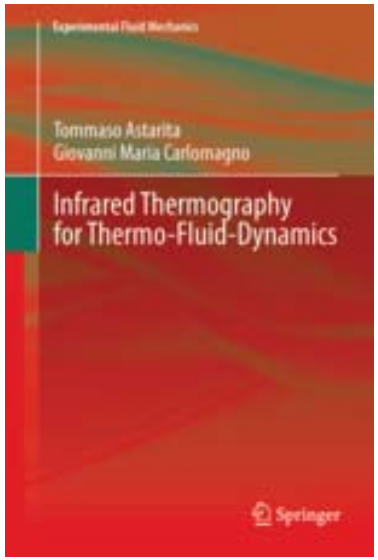

INFRARED THERMOGRAPHY IN THERMO-FLUID-DYNAMICS

Series: EXPERIMENTAL FLUID MECHANICS - Springer

Astarita *Tommaso and* Carlomagno *Giovanni Maria*

2013 - 248 p. 119 illus., 47 in color

ISBN 978-3-642-29507-2

ISBN 978-3-642-29508-9 (eBook)

APPLIED & TECHNICAL PHYSICS. MECHANICS

ABOUT THIS BOOK

Information

- **Introduction into this very accurate surface temperature measurement method**
- **Examines a significant number of examples and applications in detail**
- **Guides both, the experienced researcher and the young student**

Infrared thermography is a measurement technique that enables to obtain non Intrusive measurements of surface temperatures. One of the interesting features of this technique is its ability to measure a full two dimensional map of an object surface temperature and, for this reason, it has been widely used as a surface flow visualization technique. Since the temperature measurements can be extremely accurate, it is possible, by using a heat flux sensor, also to measure convective heat transfer coefficient distributions on a surface, making the technique *de facto* quantitative. This book, starting from the basic theory of radiation and heat flux sensors, guides, both the experienced researcher and the young student, in the correct application of this powerful technique to study convective heat transfer problems. A significant number of examples and applications are also examined in detail, often pointing out some relevant aspects.

Table of contents:

Introduction and Historical Groundings - Physical Background - Infrared Scanner - Heat Flux Sensors - Restoration of Thermal Images - Some Practical Considerations - Applications.

10.21611/qirt.2016.d

MEASUREMENTS OF HEAT FLUXES

Measuring heat fluxes from a stream to a surface is one of the main and difficult issues of ***thermo-fluid-dynamics***.

Measuring heat fluxes involves measuring temperatures.

The temperature has to be measured in ***heat flux sensors*** (generally slabs).

The appropriate equation for heat conduction in solids, applied to the ***selected sensor model***, yields the relationship by which the measured temperature is correlated to the heat transfer rate.

The use of an infrared camera as ***temperature detector*** is beneficial when compared to standard detectors.

- Entirely **two-dimensional detector** (allows the evaluation of ***heat flux variations*** and of ***errors due to tangential conduction*** along the sensor).
- **Non intrusive** (avoids the errors due to ***thermal conduction through thermocouples, or RTD's connections***).

10.21611/qirt.2016.d

UNSTEADY HEAT FLUX SENSORS

THIN SKIN - The thin skin is based on the assumption that a thin slab constituting the sensor behaves as an ***ideal calorimeter*** which is ***isothermal across its thickness***.
Heat flux uniformly increases the slab temperature with time.

$$Q_w = Q_c - Q_r$$

$$Q_w = \rho c s \frac{dT}{dt}$$

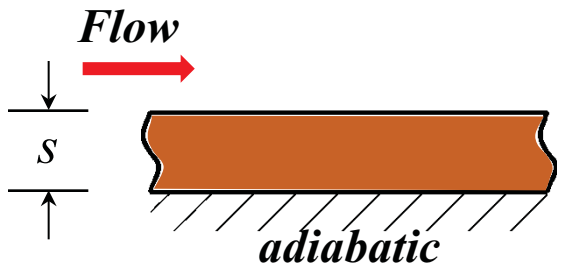

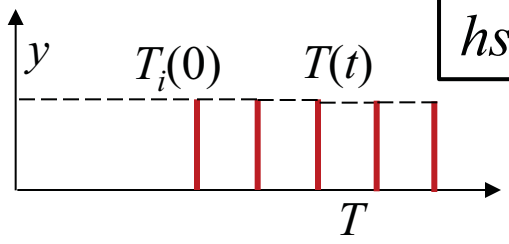

$$hs/\lambda << 1$$

THIN FILM - The thin film is based on the ***theory of heat conduction in a semi-infinite wall.***
Heat flux steadily increases the slab ***surface*** temperature $T(t,0)$.

$$Q_w = const$$

$$T(t,0) - T_i = \frac{Q_w}{2}\sqrt{\frac{t}{\pi \rho\, c\, k}}$$

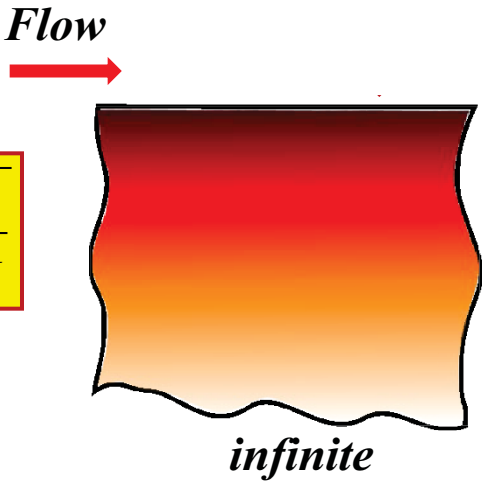

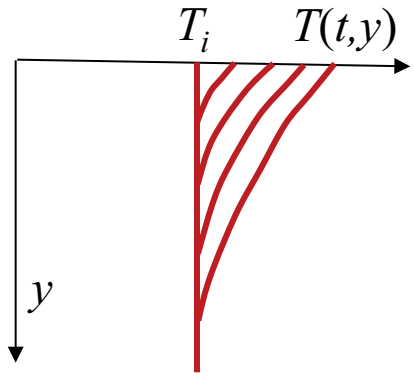

10.21611/qirt.2016.d

HEATED THIN FOIL (STEADY)

It consists of ***heating a thin metallic foil*** (AISI 40μm thick), ***or a printed circuit board, by Joule effect*** and, by measuring the foil temperature, computing the heat transfer coefficient ***h*** between the foil and the stream.

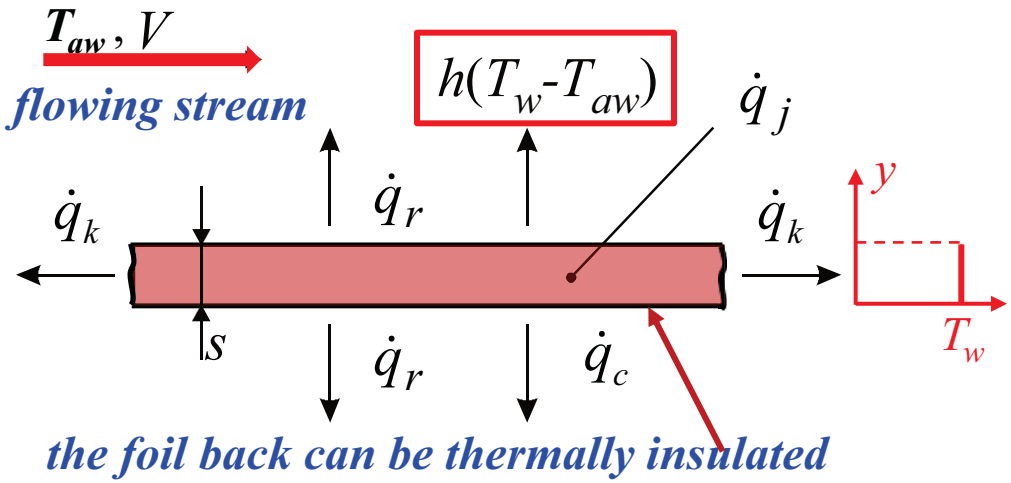

- $\dot{q}_j$ is the **known** ***Joule heating***
- $\dot{q}_r$ are the losses due to radiation
- $\dot{q}_k$ are due to tangential conduction
- $\dot{q}_c$ is convection at sensor back side
- $h(T_w - T_{aw})$ is the convective flux ***to be measured***

If the Biot number is:

$$Bi = hs/\lambda << 1$$

the heated foil can be assumed ***isothermal across thickness*** and ***measurements performed on either foil side***.

The heat transfer coefficient ***h*** is inferred from the ***energy conservation equation***:

$$h = \frac{\dot{q}_j - \dot{q}_r - \dot{q}_k - \dot{q}_c}{T_w - T_{aw}}$$

10.21611/qirt.2016.d

IMPINGING JETS (*heated thin foil*)

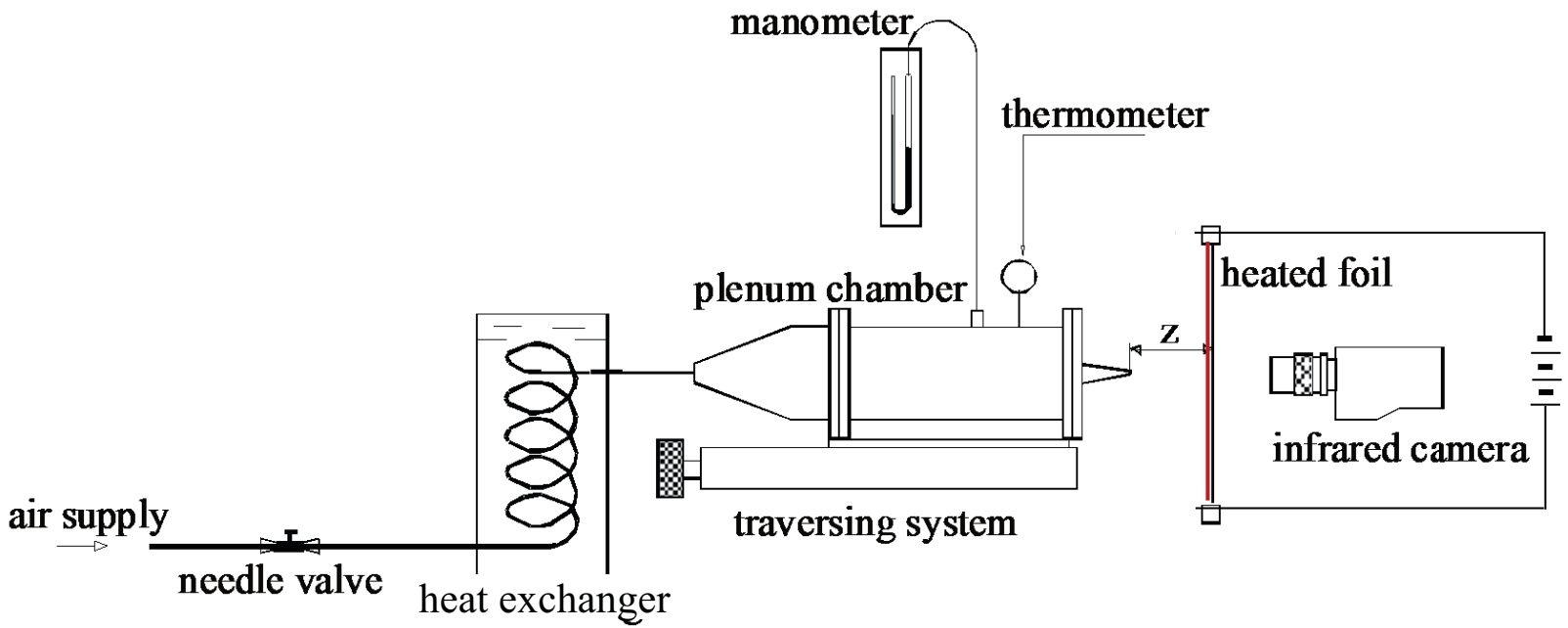

EXPERIMENTAL ARRANGEMENT FOR IMPINGING JETS

The heated foil consisted of a 40μm AISI 304 foil

10.21611/qirt.2016.d

AGA 780
100x100 px

Jet impinging on a plate, contours of constant temperature; *z/d*=6, *Re*=28000 (1986).

To my knowledge, shows the first thermographic image of an impinging jet.

10.21611/qirt.2016.d

RECOVERY FACTOR

$$r = \frac{T_{aw} - T_{\infty}}{T_o - T_{\infty}}$$

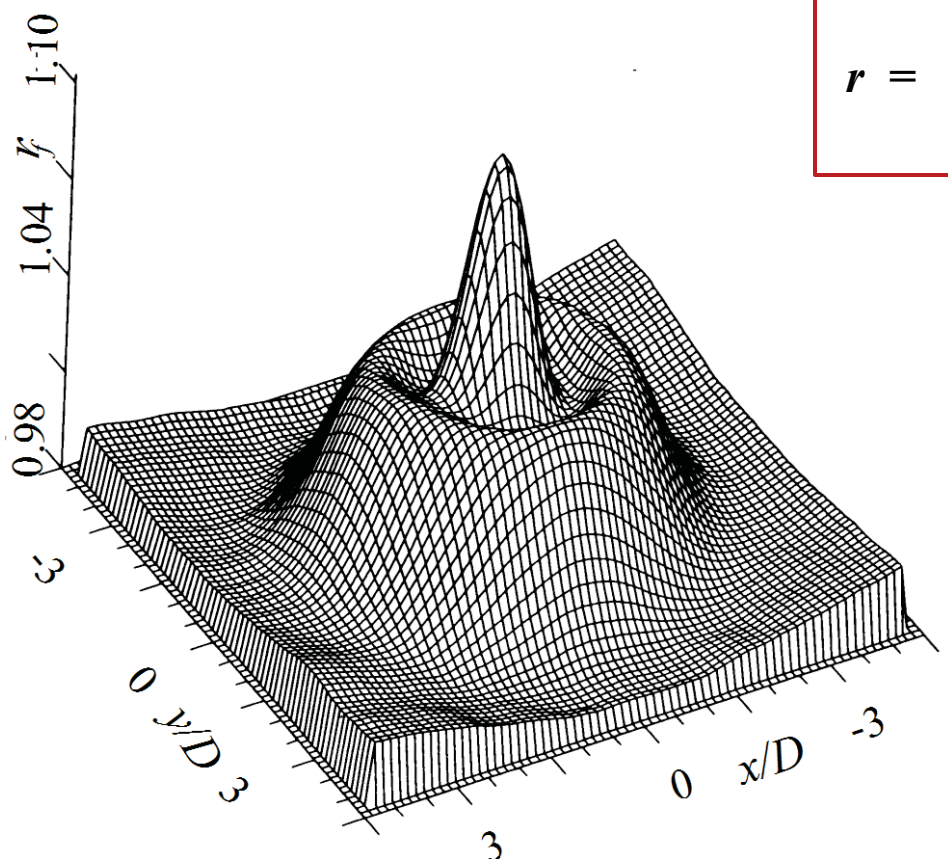

RELIEF MAP OF THE RECOVERY FACTOR OF A JET IMPINGING ON A FLAT PLATE FOR D = 10mm, z/d = 2 AND M = 0.52 (1991)

10.21611/qirt.2016.d

NUSSELT NUMBER

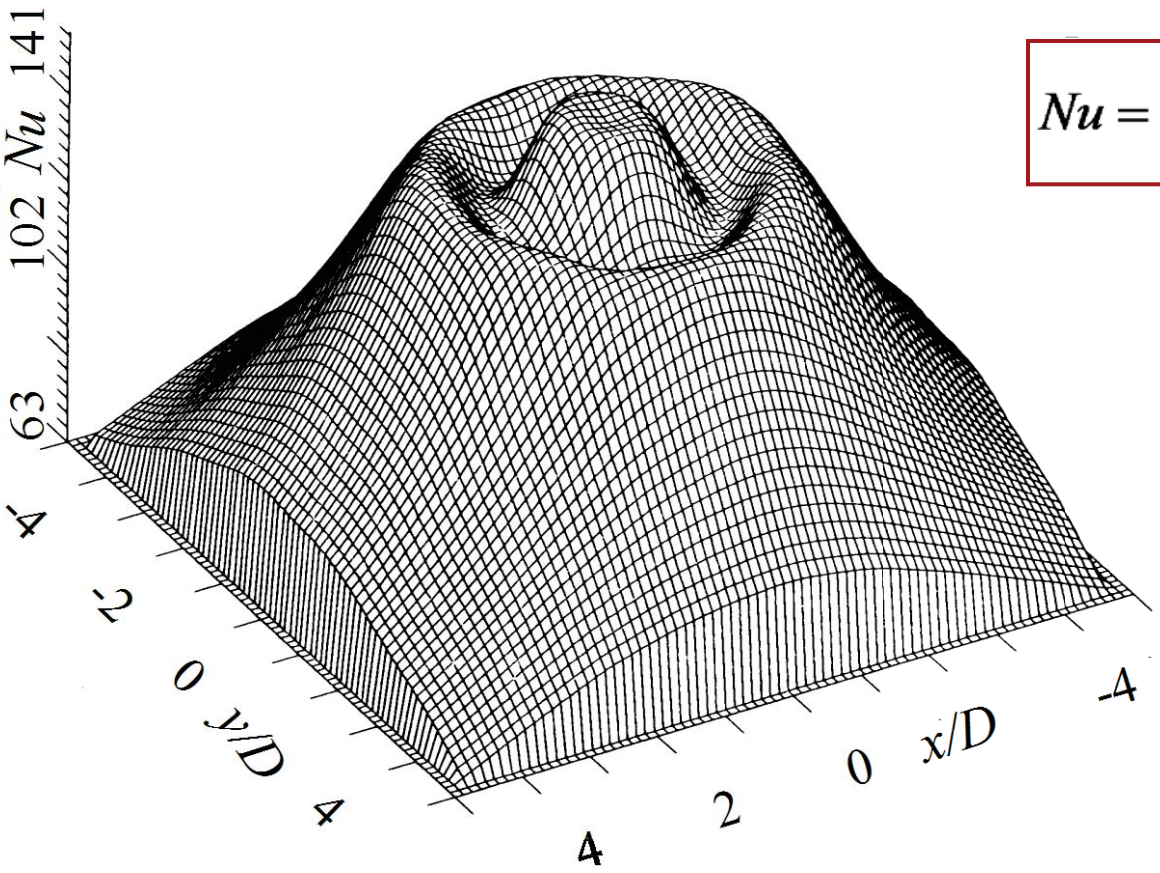

$$Nu = \frac{hD}{k}$$

RELIEF MAP OF THE NUSSELT NUMBER OF A SINGLE JET IMPINGING ON A FLAT PLATE FOR D =10mm, $z/d = 2$ AND Re_D = 28,000 (1991)

In a 1990 technical meeting in Kozubnik (Bielsko-Biała, prof. Fisdom), I was asked if these plots originated from numerical computations !!!

10.21611/qirt.2016.d

SHEAR LAYER INSTABILITY

In the meantime, Meola et al. (1995), through measurements of ***adiabatic wall temperature***, observed instability developing for high M values.

E.g., for $z/d = 4$, as the Mach number M increases, the vortex ring, which is located in the shear layer at $r = 1.2\ d$ (r indicates the radial coordinate), strengthens and breaks up (***Widnall instability***), entailing entrainment of warmer ambient air and giving rise to the formation of azimuthal structures.

Meola C., de Luca L. and Carlomagno G.M., (1995) Azimuthal instability in an impinging jet - adiabatic wall temperature distribution, *Exp Fluids,* 18(5):303–310

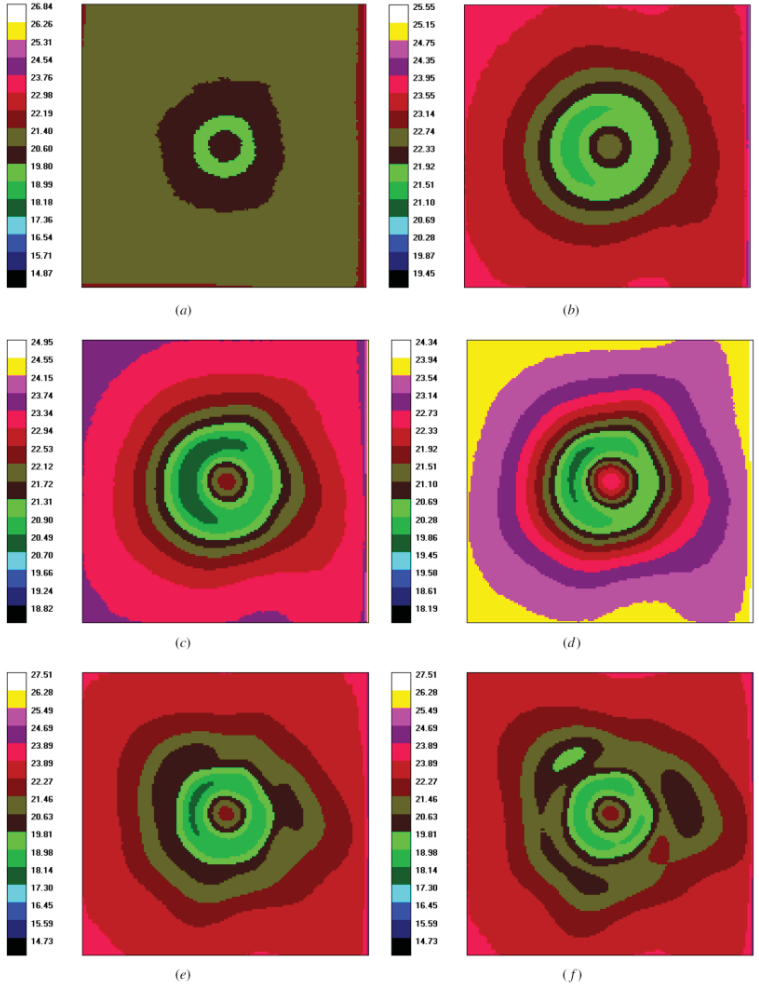

Variation of adiabatic wall temperature with the Mach number for $d = 5$ *mm*, $z/d = 4$; *(a)* $M = 0.3$; *(b)* $M = 0.4$; *(c)* $M = 0.5$; *(d)* $M = 0.56$; *(e)* $M = 0.67$; *(f)* $M = 0.71$

10.21611/qirt.2016.d

HYPERSONIC FLOW

10.21611/qirt.2016.d

SURFACE FLOW ON A DOUBLE ELLIPSOID MODEL

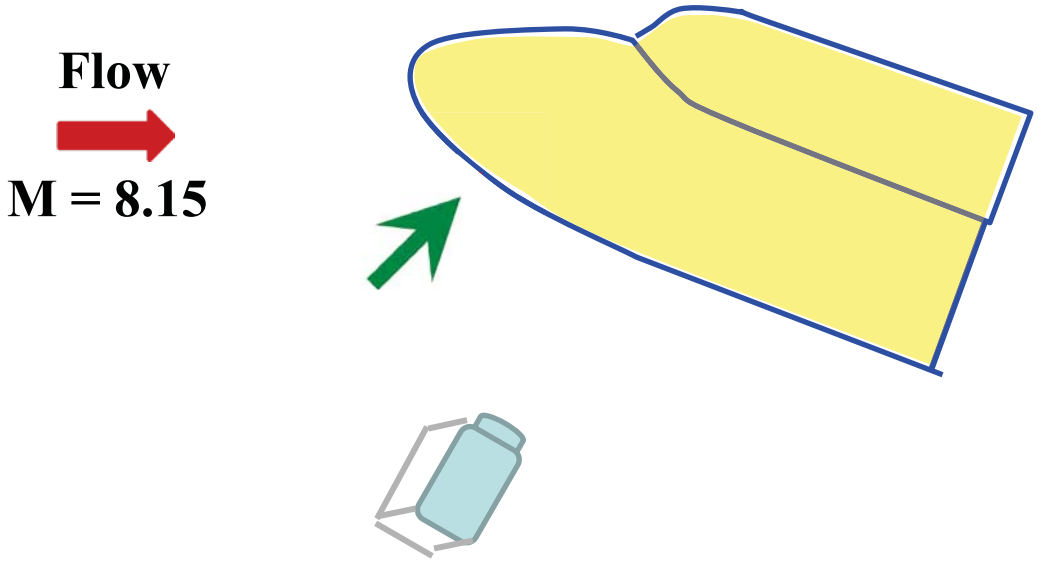

The model is suddenly exposed to a high enthalpy hypersonic stream at M = 8.15 (CEAT, Poitiers) and thermal images of the windward (bottom) side are recorded as a function of time.

Several trip cylindrical wires (0.5*mm* high, 0.22*mm* in diameter and placed at 5*mm* steps) are implanted 30*mm* away from the ellipsoid nose.

10.21611/qirt.2016.d

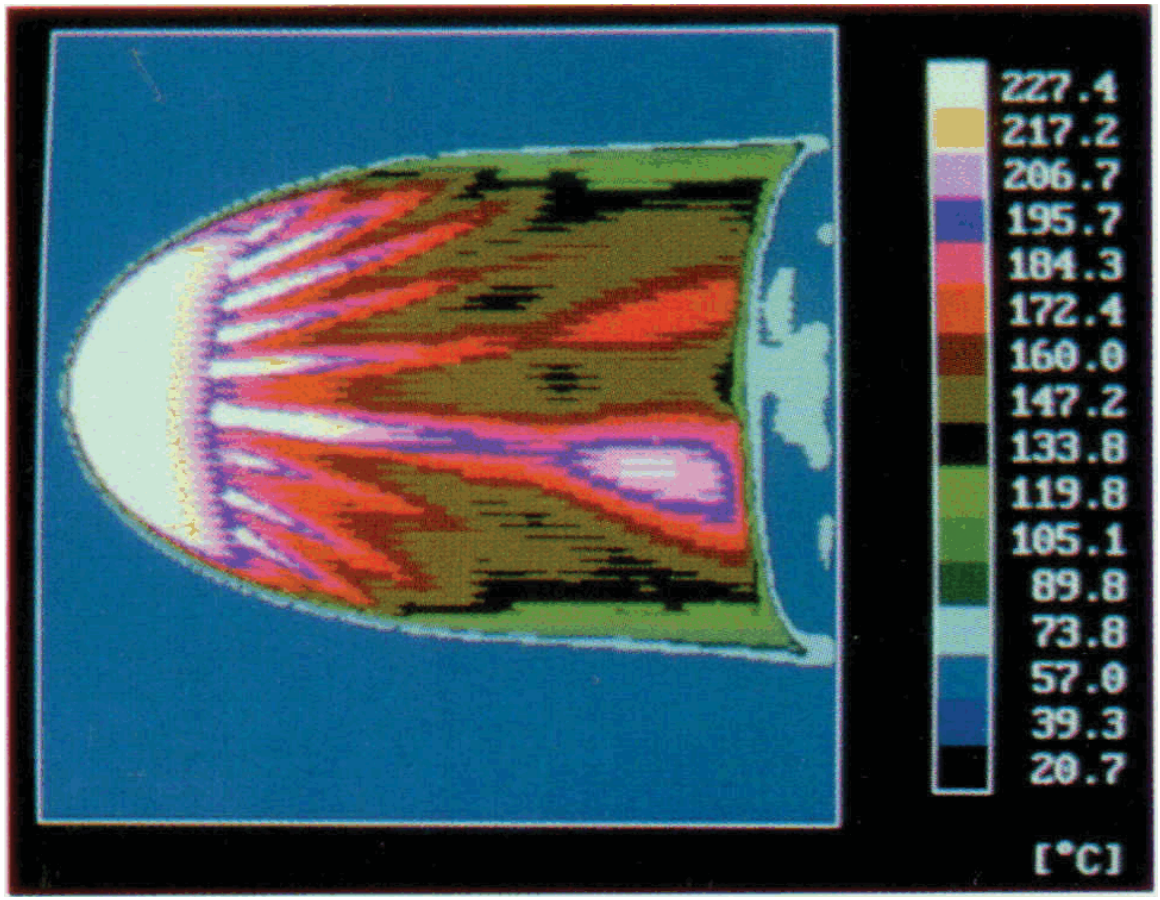

Flow from left to right

Temperature map of the ***windward side*** of a double ellipsoid model at $M = 8.15$, $\alpha = 30°$, $0.48s$ after model injection. Wires wakes are clearly visible.

DE LUCA L, CARDONE G, CARLOMAGNO G.M., DE LA CHEVALERIE D.A. and DE ROQUEFORT T.A., Flow visualization and heat transfer measurement in a hypersonic wind tunnel**,** ***Exp. Heat Transf.***, Vol. 5, pp. 65-78. (1992)

10.21611/qirt.2016.d

HYPERSONIC FLOW OVER A FLAT PLATE FOLLOWED BY A RAMP

(e.g., heat transfer in re-entry problems; thin film)

CARDONE G., IR Heat Transfer Measurements in Hypersonic Plasma Flows, ***QIRT J***, **4**, 233-251 (**2007**)

10.21611/qirt.2016.d

HEAT FACILITY

High ***E***nthalpy ***A***rc-heated ***T***unnel, Centro Spazio (PISA), Italy

Main characteristics are:

- Blow-down tunnel
- Test duration: 20 - 300*ms*
- Mach number: 6
- Total Temperature: 300 - 4000*K*
- Total Entalpy: 0.3 - 6*MJ/kg*
- Reynolds Number: 10^{4}-$10^{6}/m$
- Fluids: air, helium, argon, CO2

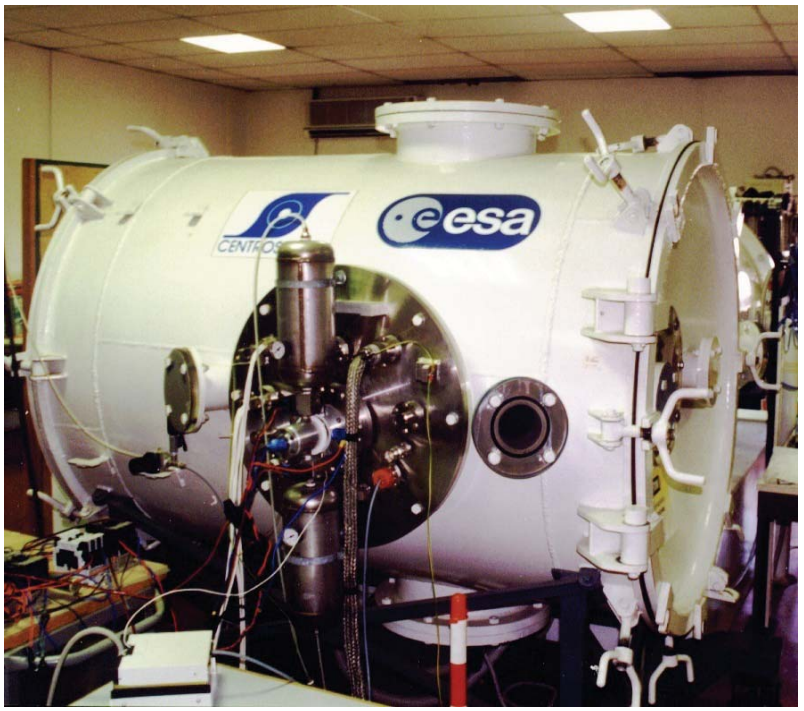

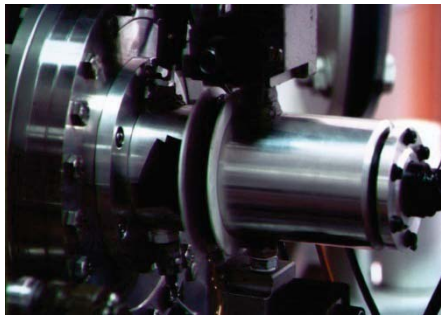

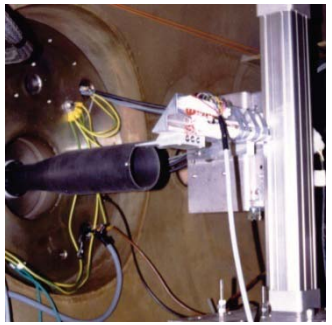

10.21611/qirt.2016.d

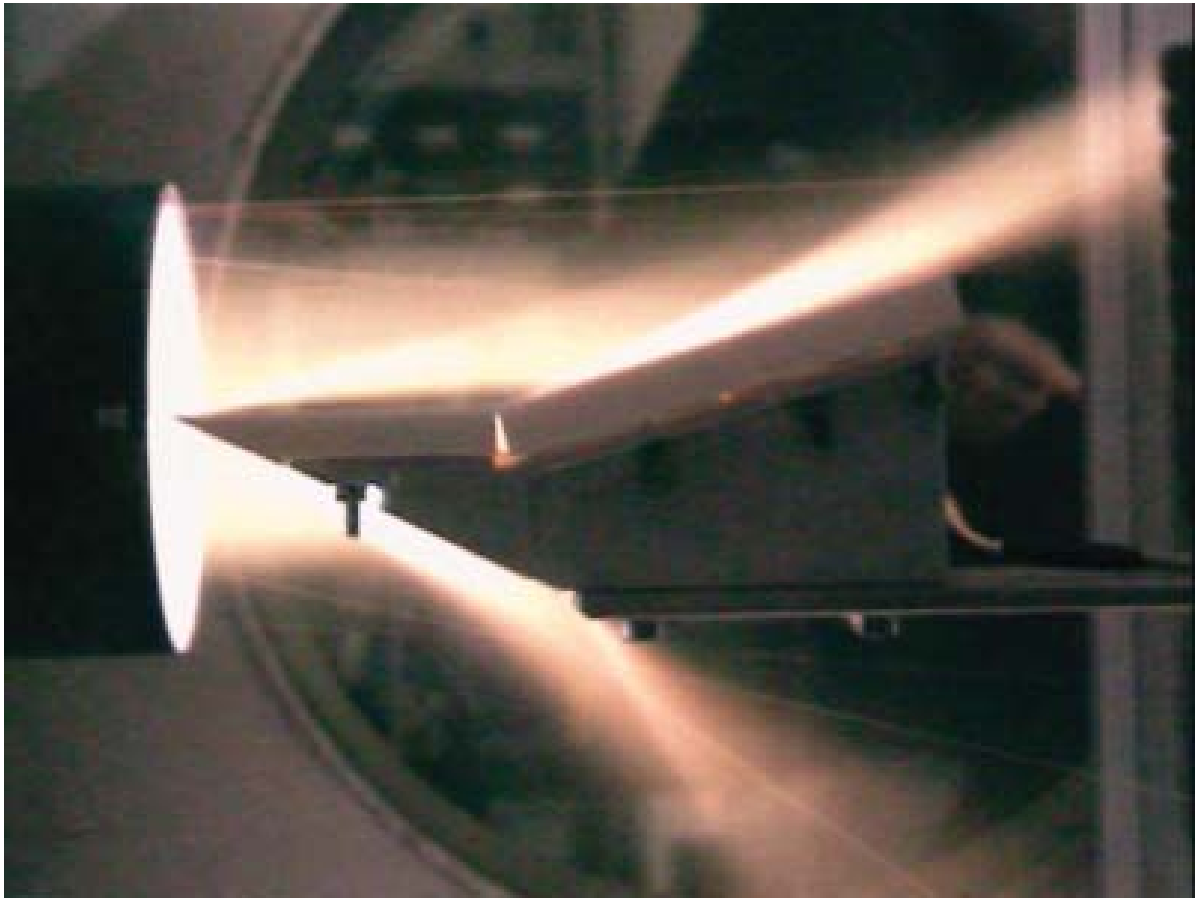

FLAT PLATE WITH 15° RAMP IN A $M = 6$ HYPERSONIC FLOW

10.21611/qirt.2016.d

FLAT PLATE WITH 15° RAMP

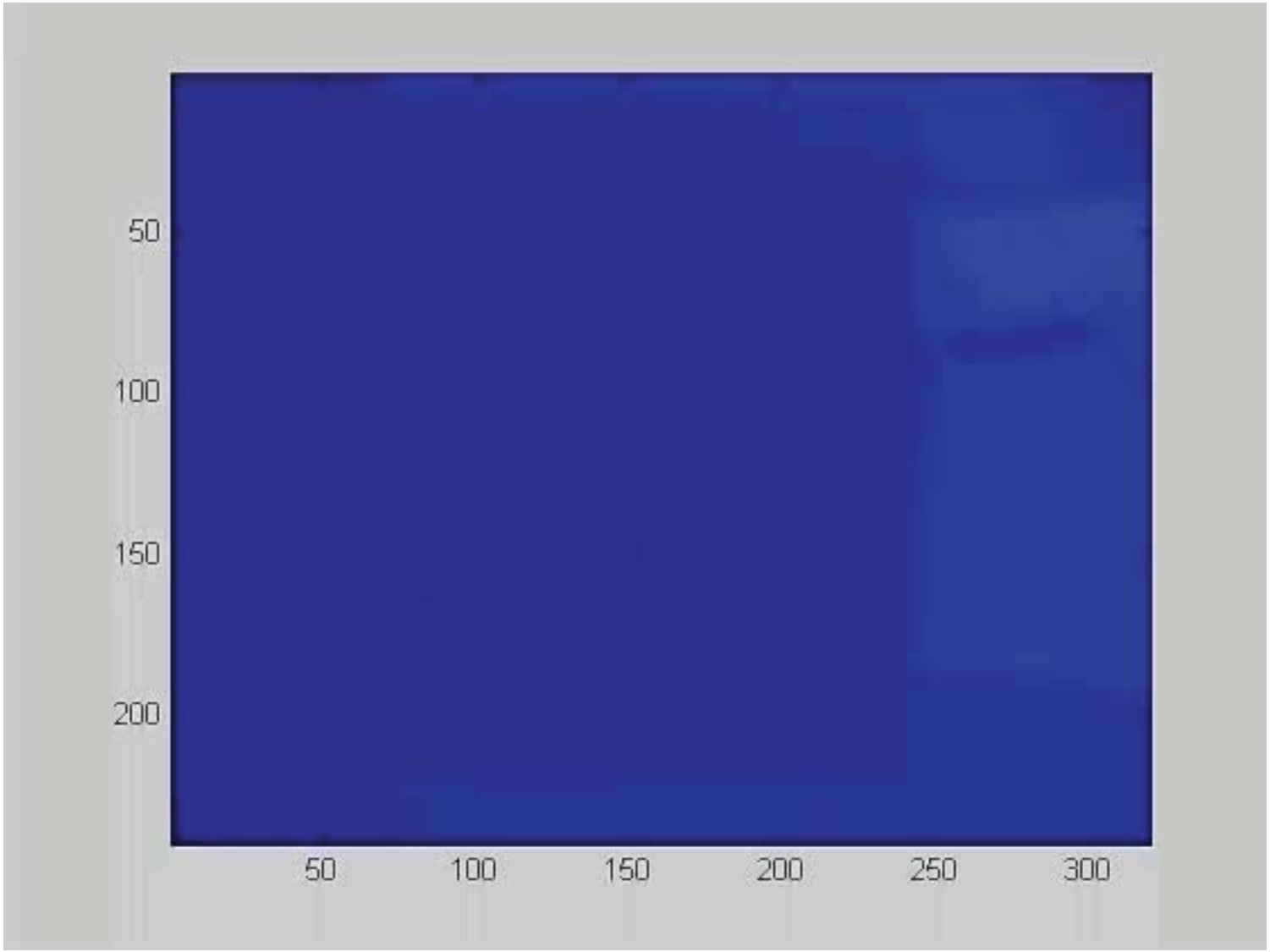

Flow from left to right

Leading edge

Hinge line

$M = 6$

10.21611/qirt.2016.d

FLAT PLATE WITH 15° RAMP

Nominal conditions $H_o = 1.8 MJKg$; $P_o = 6 bar$

Centerline data

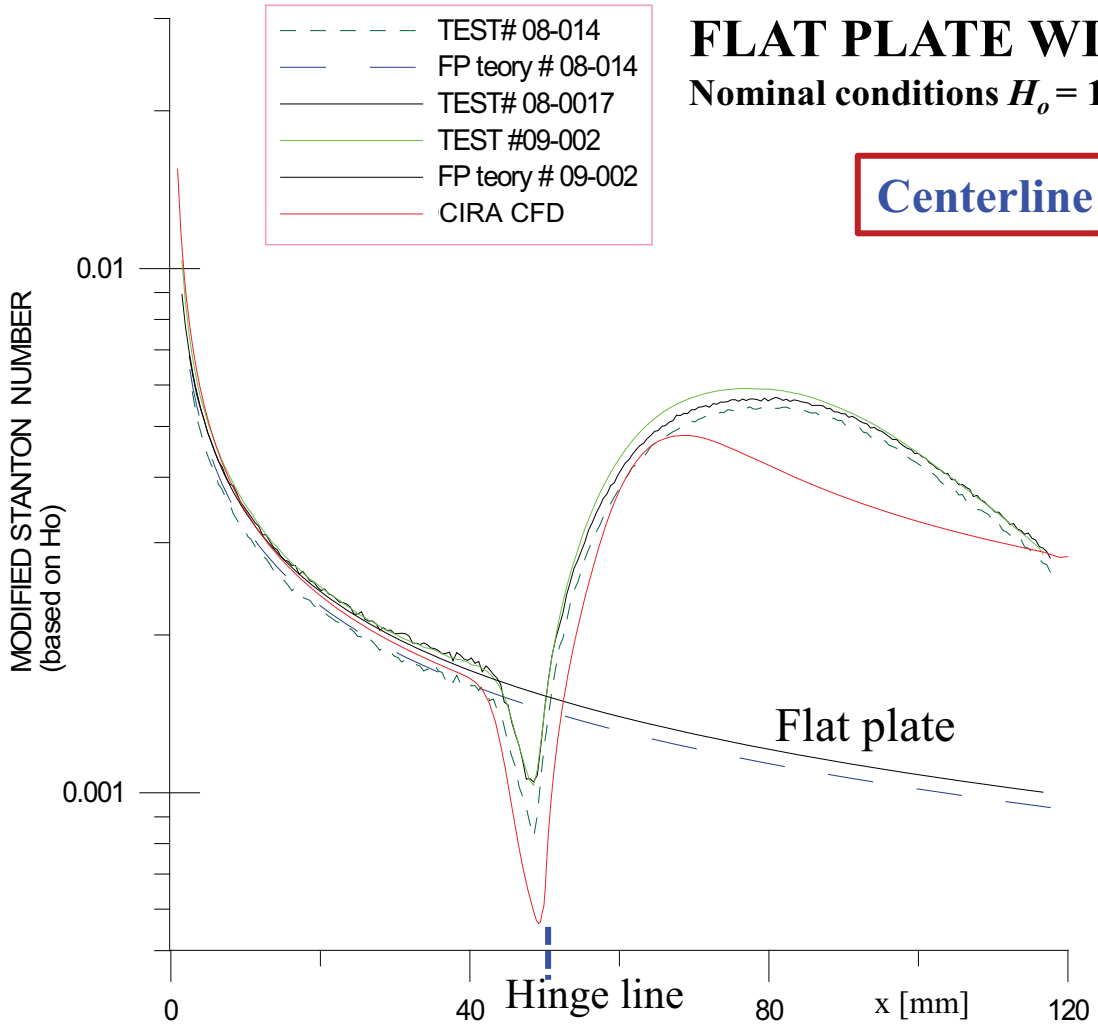

10.21611/qirt.2016.d

1990

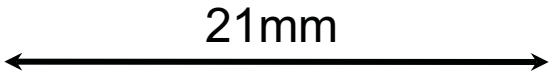

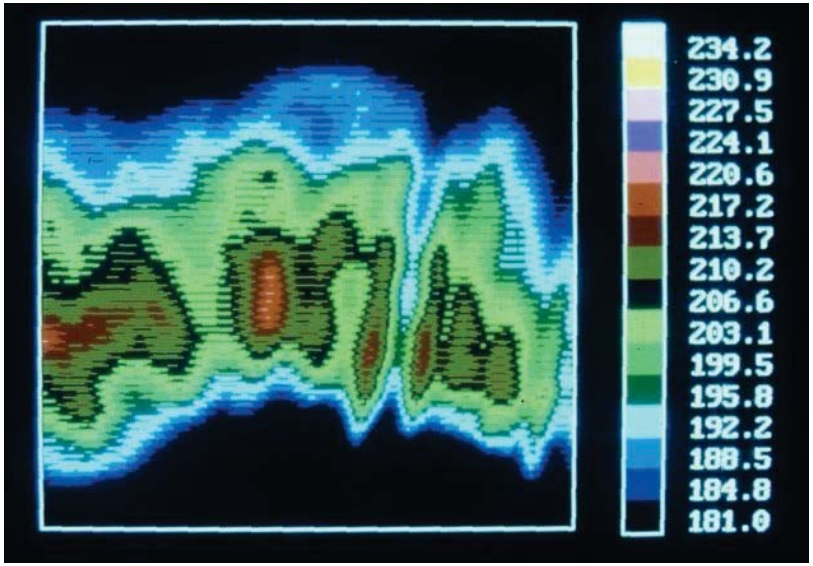

a)

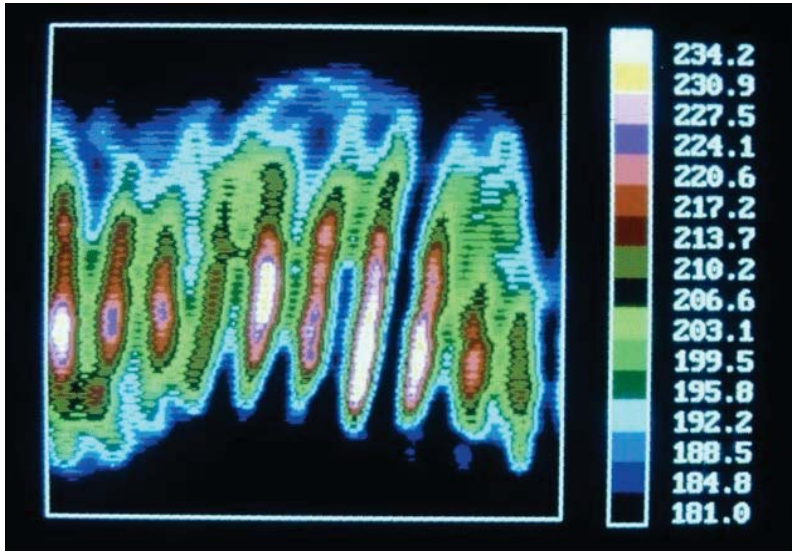

b)

Images of Goertler vortices (fluiddynamic instability) on a 30°ramp in a hypersonic flow at $M = 8.15$ (***thin-film sensor***; AGA 780):

a) ***coarse (acquired) image;***

b) ***sensor and camera restoration.***

10.21611/qirt.2016.d

PICCOLO TUBE
(DE-ICING OF A WING LEADING EDGE)
(*heated thin foil*)

MEOLA C., CARLOMAGNO G. M., RIEGEL E. and SALVATO F., An experimental study of an anti-icing hot air spray-tube system, 19th Congr. Int. Council Aeronaut. Sci., ICAS-94-2.7.1, Vol. 3, pp. 2345-2351, Anaheim, (1994).
IMBRIALE M, IANIRO A, MEOLA C and CARDONE G, Convective heat transfer by a row of jets impinging on a concave Surface, ***Int. J. Thermal Sci.*, 75**, 153-163 (2013)

10.21611/qirt.2016.d

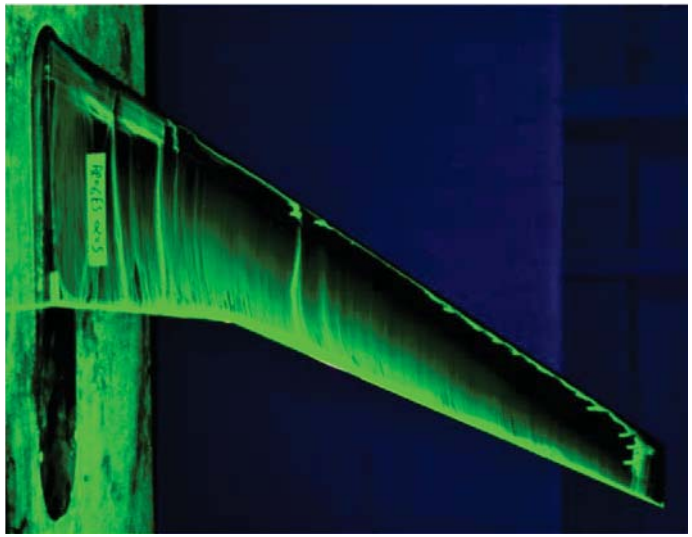

No ice

Ice formation and accretion

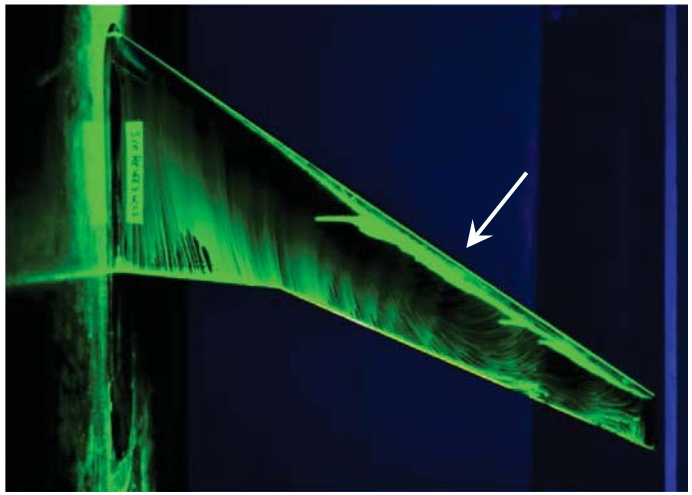

With ice

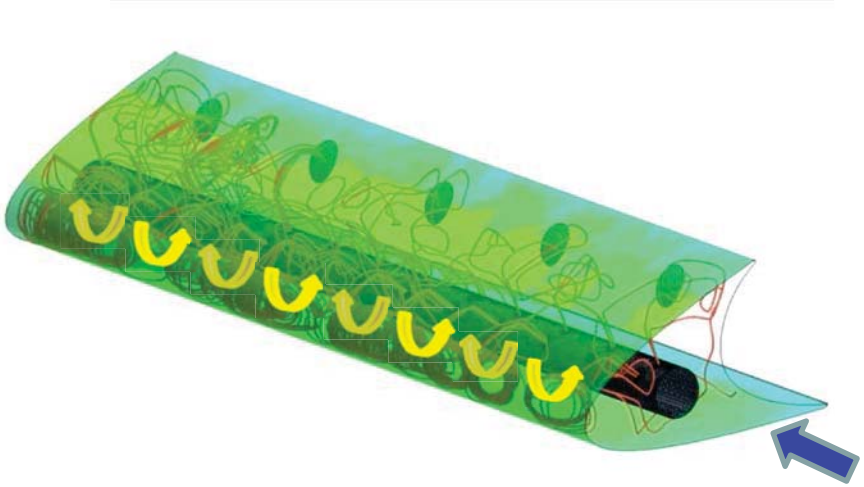

Wing with de-icing piccolo tube

10.21611/qirt.2016.d

EXPERIMENTAL APPARATUS

The test article includes the ***leading edge*** of a **NACA 0012** wing profile (1.5*m* chord), stopped at about 1/10 of the chord, with inside a spray (piccolo) tube at 4% of the chord to simulate the de-icing device.

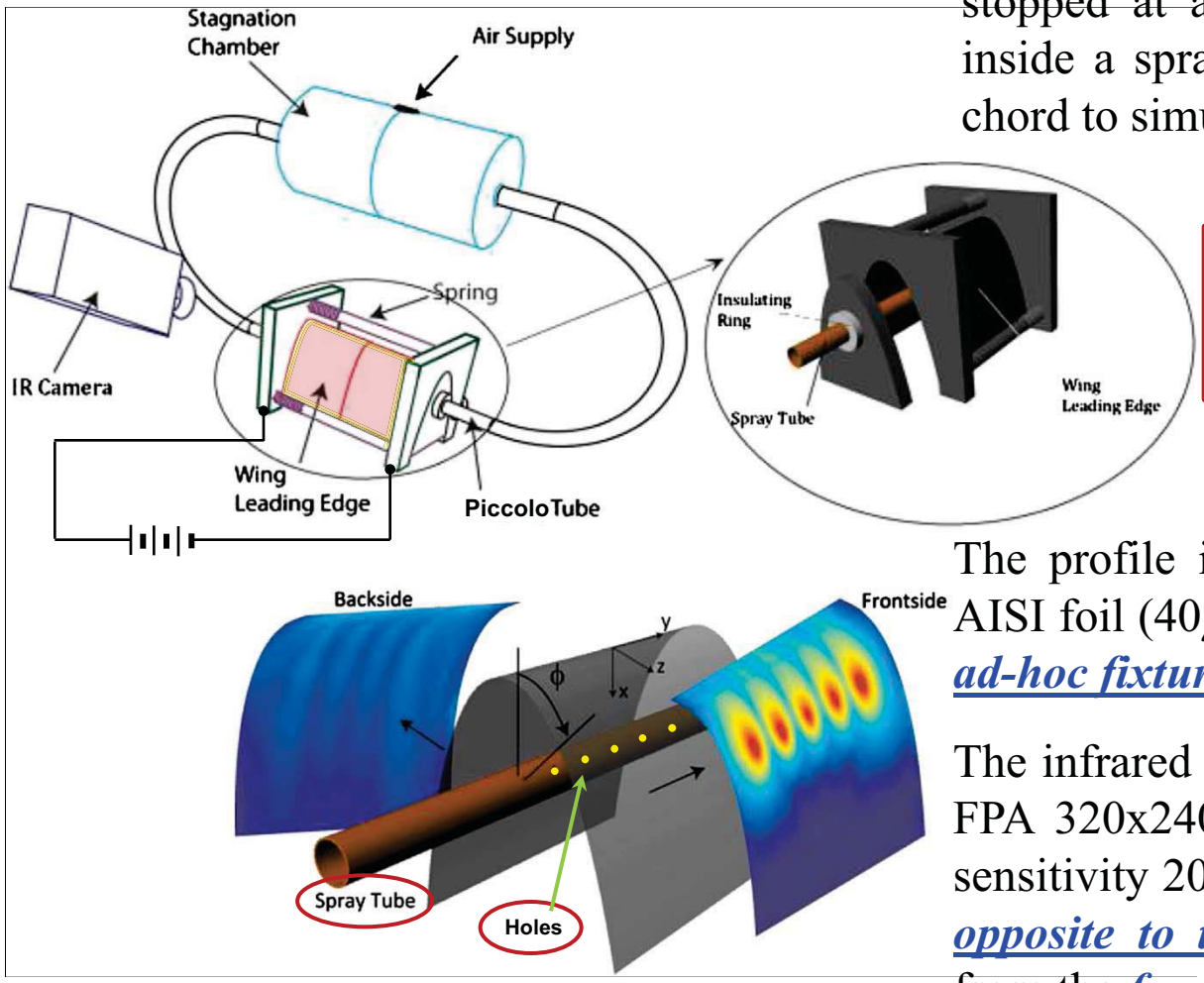

***d* and *p* are resp. *hole diameter* and *pitch*; ϕ is the *jets inclination angle* with respect to the wing chord**

The profile is 0.2*m* span-wise, made of an AISI foil (40μm thick) and lodged inside two ***ad-hoc fixtures*** to apply voltage difference.

The infrared camera (CEDIP Jade III, cooled FPA 320x240 InSb pixels, 3.8-5.3μm band, sensitivity 20mK at 300K) views the ***foil side opposite to the jet impingement one***, both from the ***front*** and the ***back***.

10.21611/qirt.2016.d

Since we are looking at a three-dimensional device, a ***geometrical camera calibration procedure***, with the thermal images of the calibration target, is necessary.

The target calibration plate is made of an Al plate, 120x120mm^2, with 17x17 (289) holes, 2.2*mm* diameter and 10*mm* deep, so to behave almost as black bodies.

The plate is moved back and forth, within measurement domain, to perform geometrical calibration.

A thermal 3D image can, therefore, be fully reconstructed.

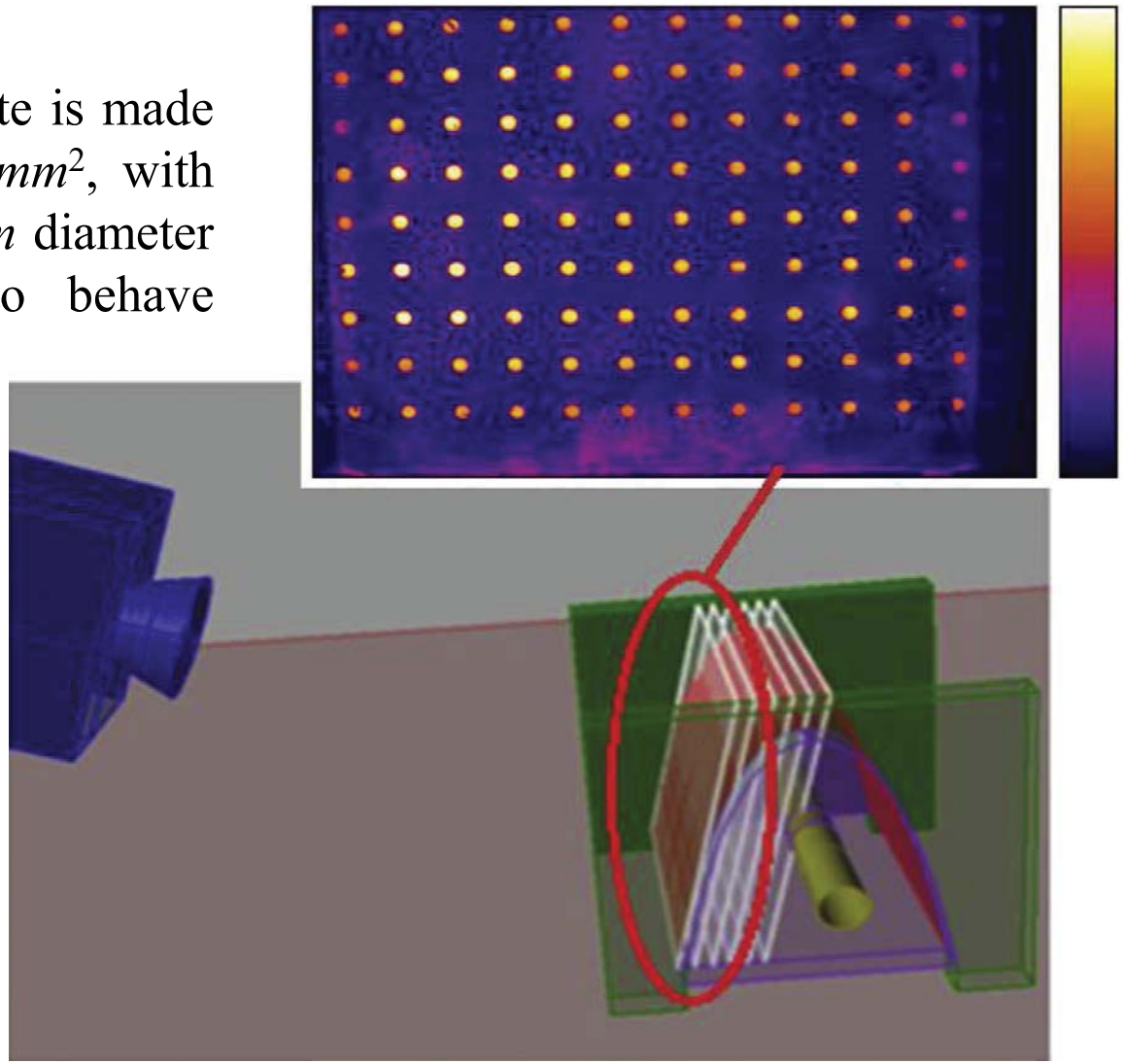

10.21611/qirt.2016.d

3D TEMPERATURE RECONSTRUCTION FOR $d = 4mm$, $\phi = 30°$, $M = 1.0$ AND $p/d = 15$:

(a) Wall temperature T_w (*with foil heating*);

(b) Adiabatic wall temperature T_{aw} (*without foil heating*).

$$\dot{q}_j = h(T_w - T_{aw})$$

$$Nu = hd/\lambda$$

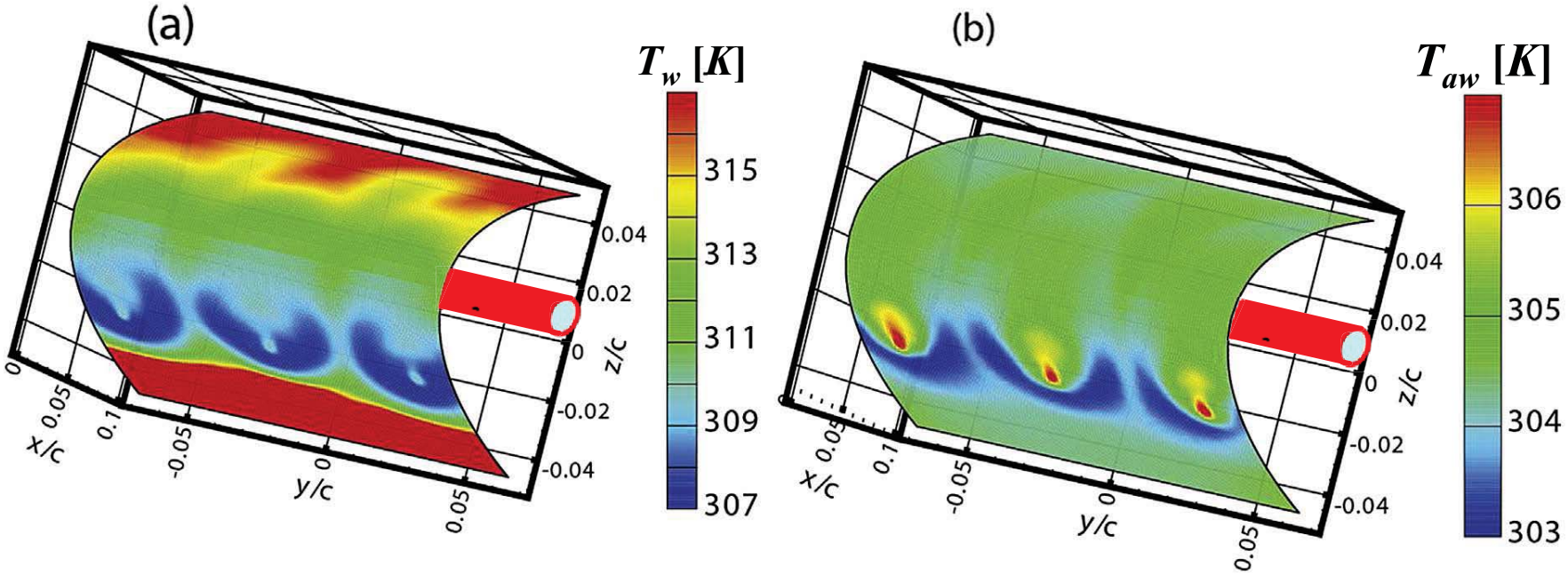

10.21611/qirt.2016.d

INFLUENCE OF JETS PITCH ON *Nu*, *M* =1.0 AND $\phi = 50°$

(a) $p/d = 5$;

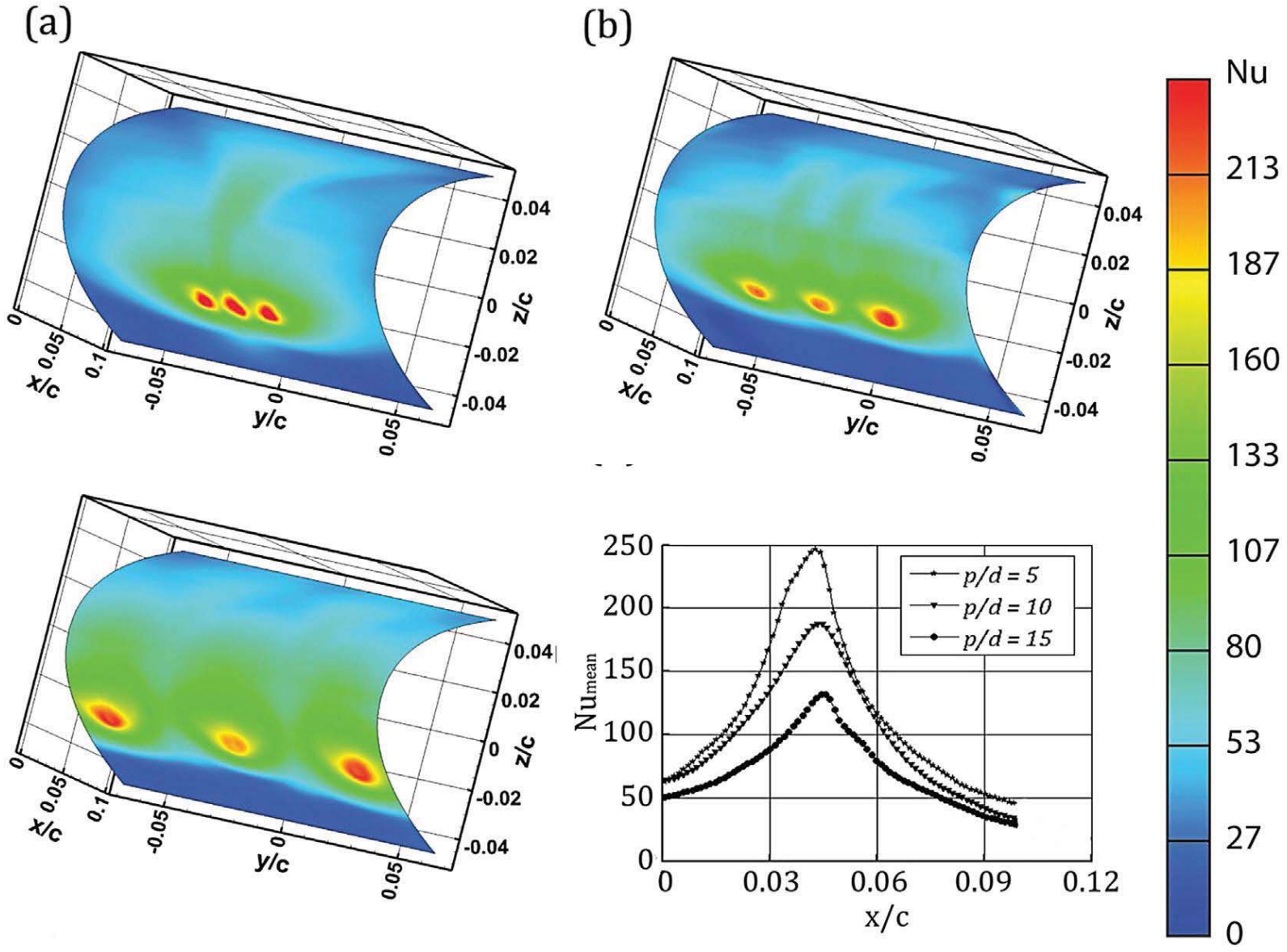

10.21611/qirt.2016.d

FLOW IN A ROTATING U CHANNEL

(*e.g., internal cooling of turbine blades; heated thin foil*)

GALLO M, ASTARITA T and CARLOMAGNO GM, Thermo-fluid-dynamic analysis of the flow in a rotating channel with a sharp U turn, ***Exp. .Fluids***, 53, 201-219 (**2012**)

10.21611/qirt.2016.d

FLOW IN A ROTATING CHANNEL

The effects of rotation, as in ***turbine blades***, change strongly the thermo-fluid-dynamic behavior of the flow in a channel.

This happens because ***in a rotating channel with an U turn*** there is interaction between the following forces:

- ***Pressure gradients causing the flow in the main direction***
- ***Coriolis forces***
- ***Centrifugal forces***

The resulting flow field is highly three-dimensional (especially in the turns) and this affects the heat transfer coefficient distribution.

This is why the problem has been studied with both ***Particle Image Velocimetry*** (***PIV***) and ***InfraRed Thermography*** (***IRT***).

10.21611/qirt.2016.d

COMPARISONS OF *Nu/Nu** DISTRIBUTIONS

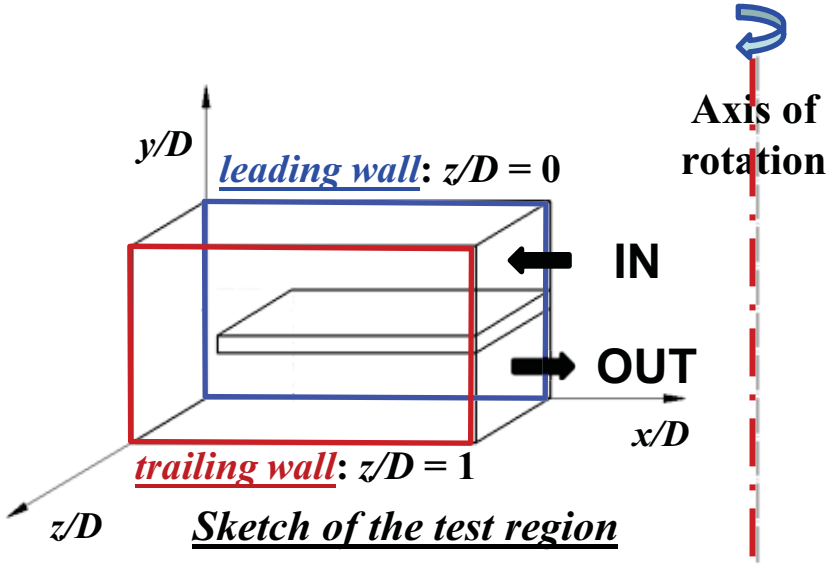

Sketch of the test region

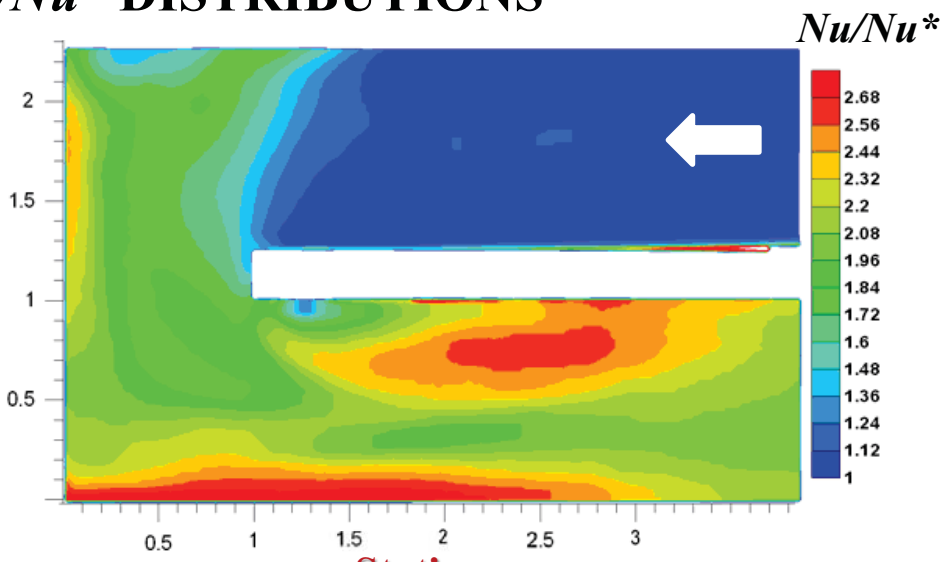

Static case

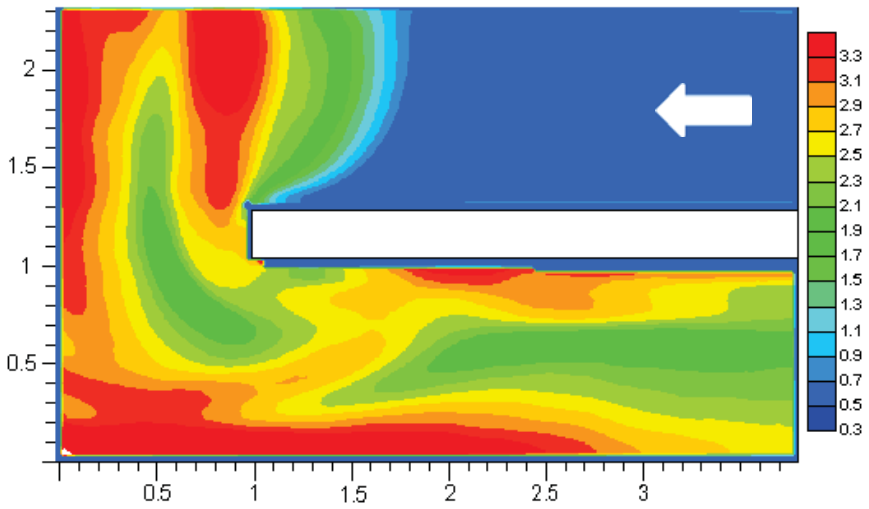

Leading wall

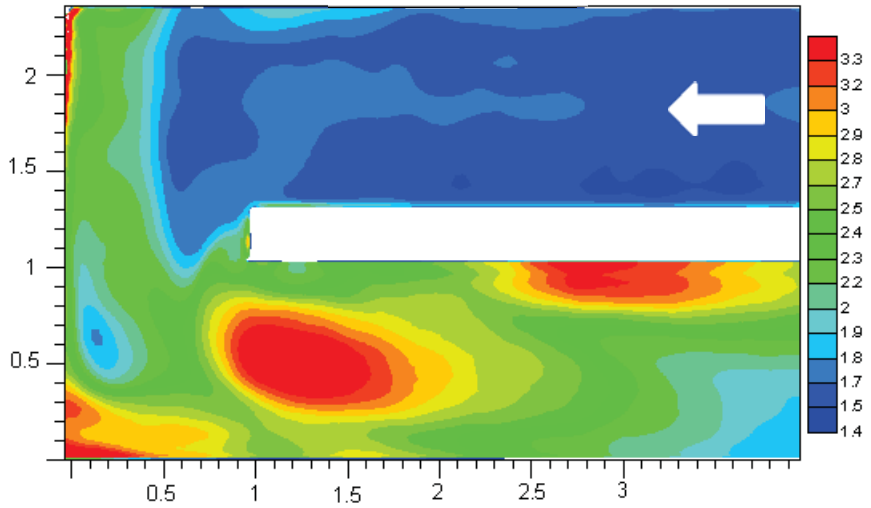

Trailing wall

$$Nu = \frac{hD}{k} \quad ; \quad Nu^* = 0.024\, Re^{0.8}\, Pr^{0.4}$$

10.21611/qirt.2016.d

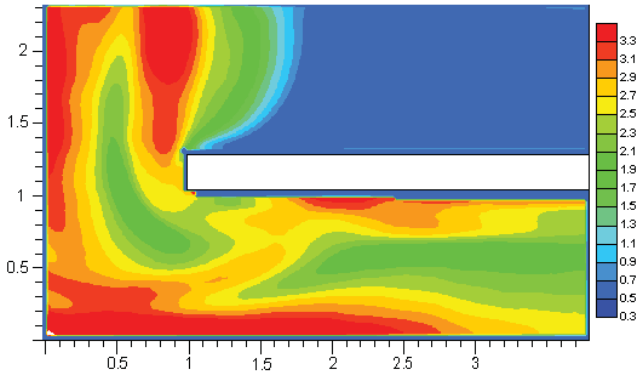

Leading wall

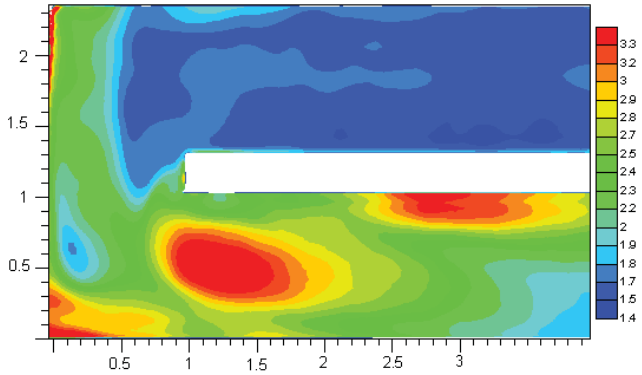

Trailing wall

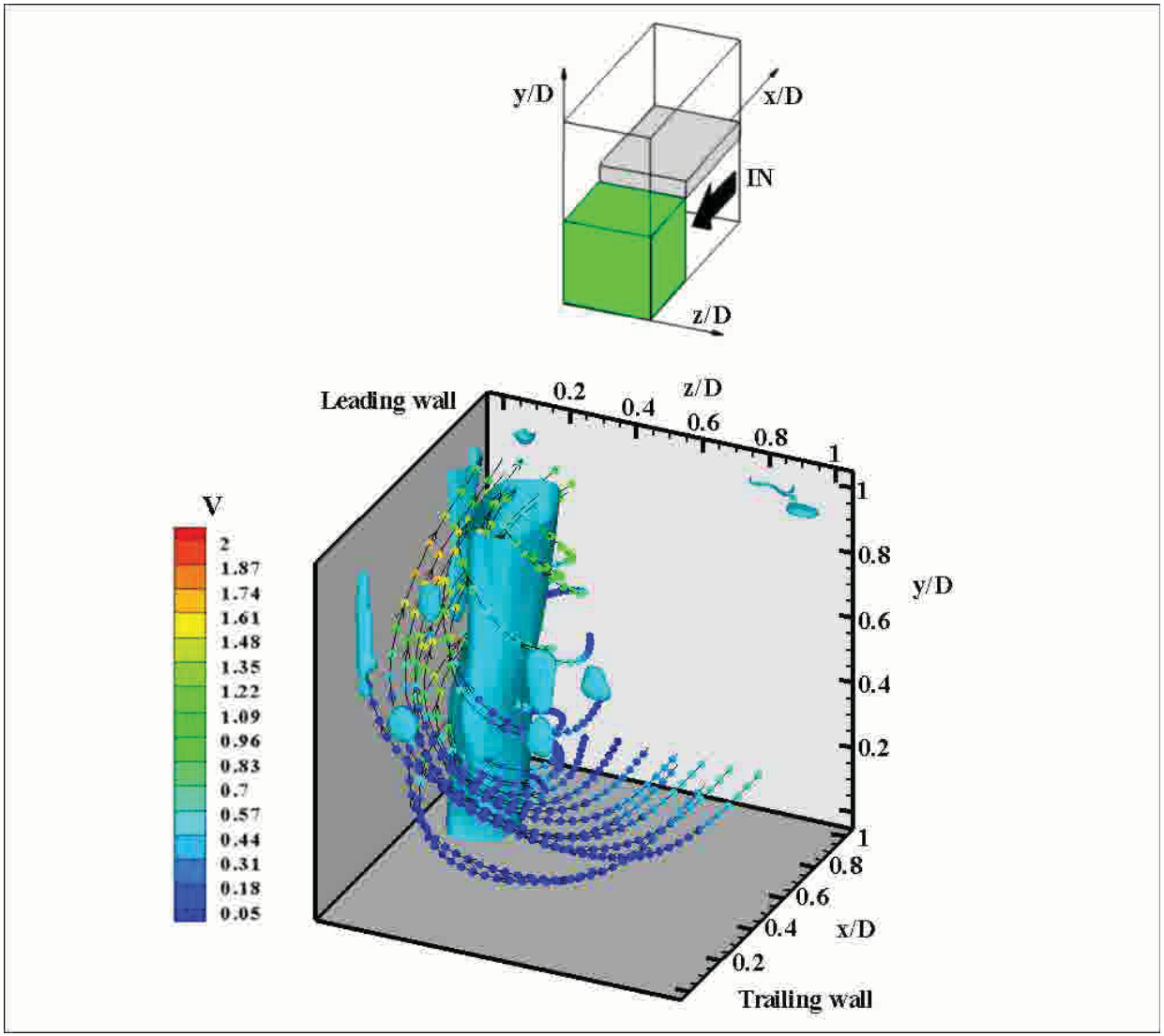

GALLO M., ASTARITA T. and CARLOMAGNO G.M., Thermo-fluid-dynamic analysis of the flow in a rotating channel with a sharp U turn, ***Exp. Fluids***, 53, 201-219 (2012)

10.21611/qirt.2016.d

IMPINGING JETS

(*e.g., for cooling purposes; heated thin foil*)

VIOLATO D, IANIRO A, CARDONE G and SCARANO F, Three-dimensional vortex dynamics and convective heat transfer in circular and chevron impinging jets, ***Int J Heat Fluid Flow***, **37**, 22–36 (2012)

10.21611/qirt.2016.d

TOMOGRAPHIC PIV (3D-3C)

Tomographic PIV is a very powerful research tool.

TomoPIV is an innovative experimental technique, based on a ***multiple camera system***, ***three-dimensional volume lighting*** and 3D reconstruction of particles velocity field within the ***whole measurement volume***.

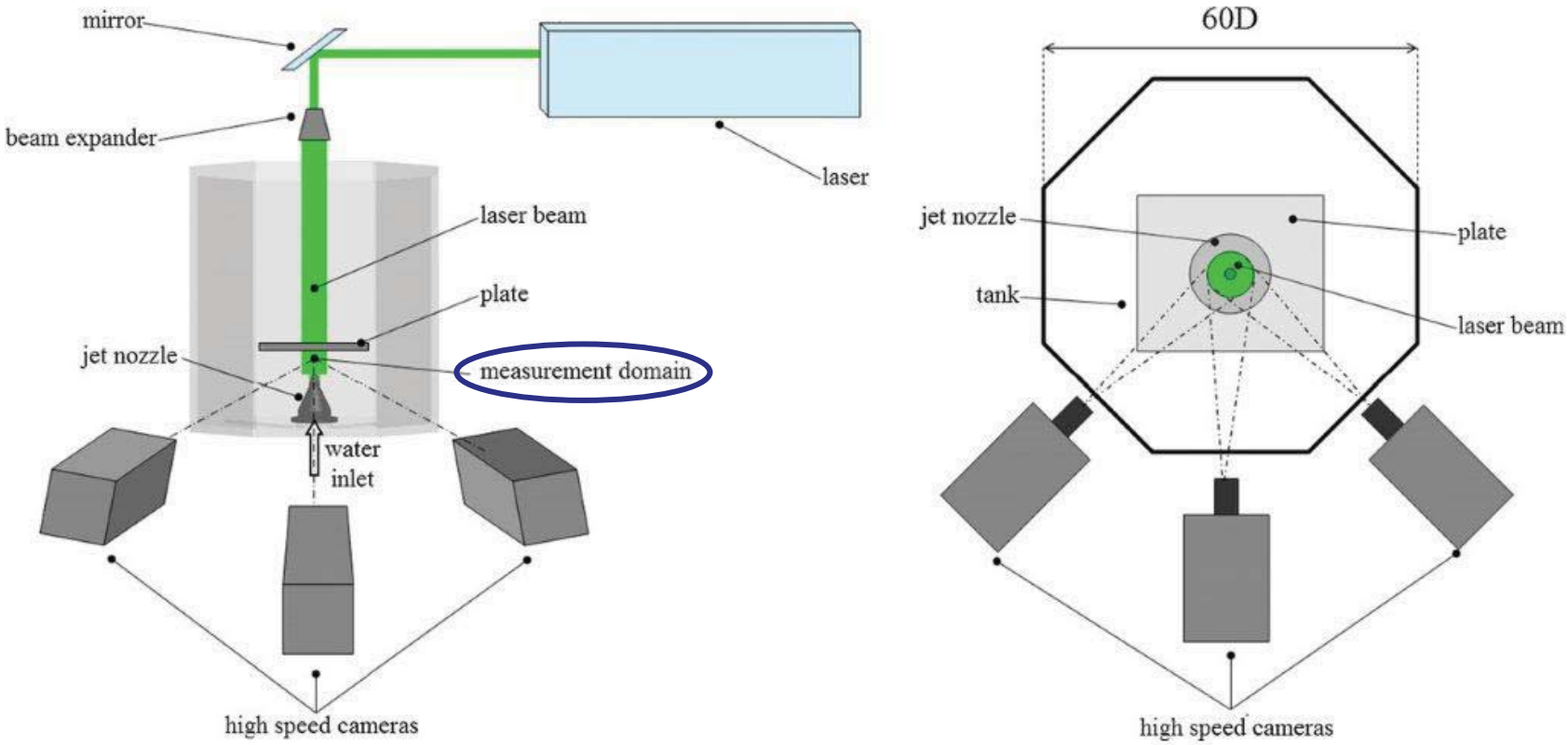

Tomographic PIV experimental apparatus for impinging jets

10.21611/qirt.2016.d

TOMOGRAPHIC PIV (3D-3C)

Tomographic PIV is a ***time-resolved*** research tool.

Besides what is encountered in standard nozzles, ***chevron nozzles*** generate ***azimuthal instabilities***, ***already in the jet shear layer***, which induce an ***increase of the heat transfer in the impingement region***. The noise they produce is much lower.

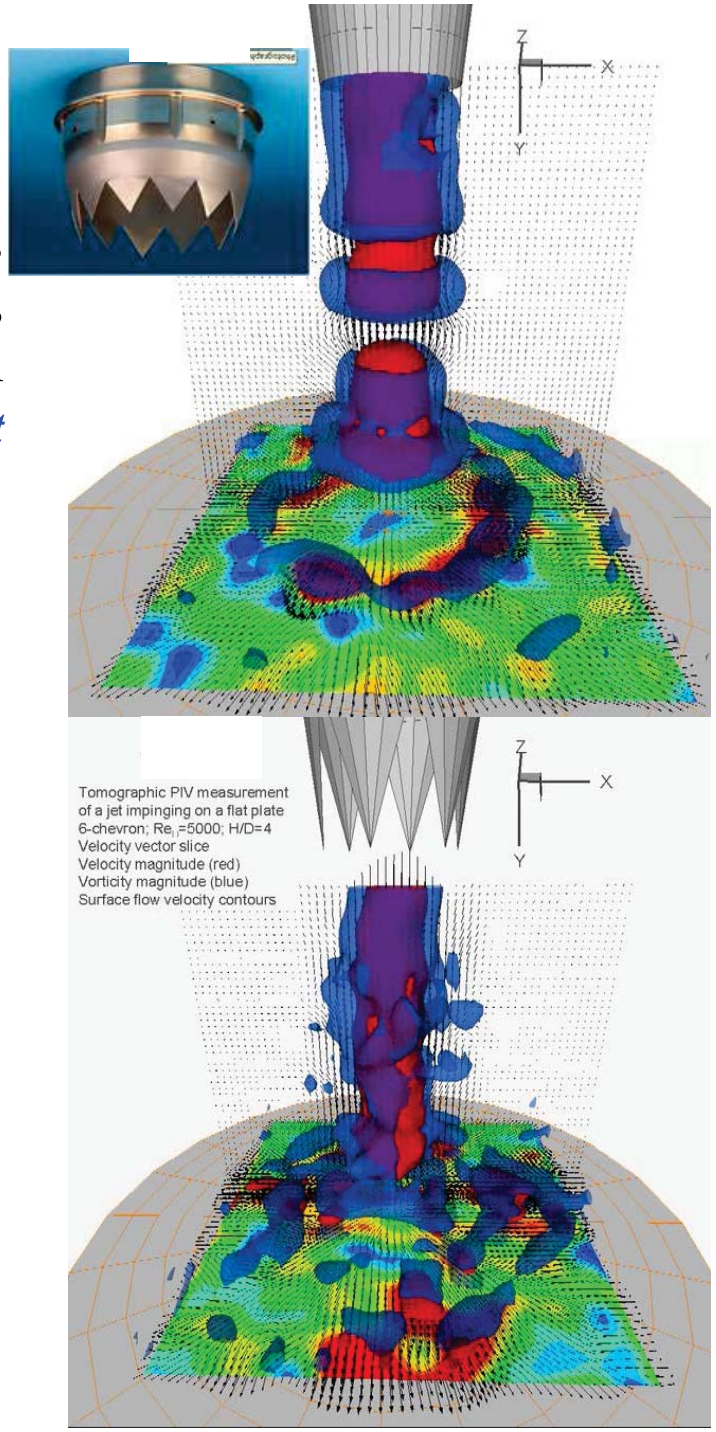

standard nozzle ***chevron***

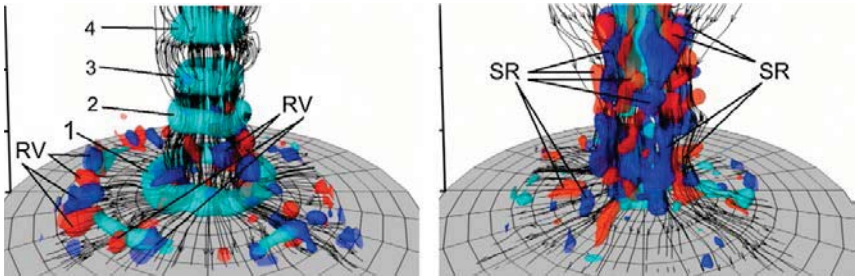

RV radial vortices ***SR streamwise structures***

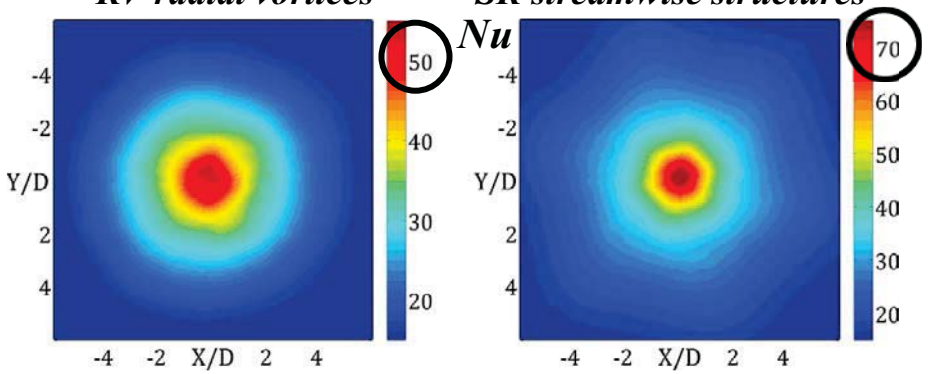

VIOLATO D, IANIRO A, CARDONE G and SCARANO F, Three-dimensional vortex dynamics and con-vective heat tran-sfer in circular and chevron impinging jets, ***Int. J. Heat Fluid Flow***, **37** (2012) 22–36

10.21611/qirt.2016.d

ONSET OF HORIZONAL NATURALCONVECTION

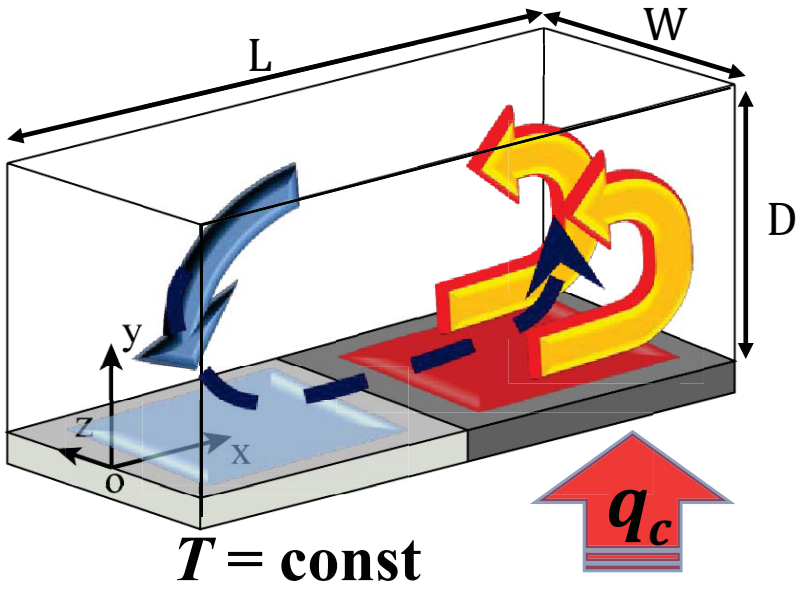

$$q_c=\lambda\frac{\partial T}{\partial y}\approx\alpha\rho c_p\frac{\Delta T}{L}$$

Main dimensionless parameters:

- Prandtl number $Pr=\nu/\alpha$;
- Rayleigh number $Ra_L=Pr\cdot Gr_L=\frac{\beta\Delta T g L^3}{\nu\alpha}$; $\Rightarrow$ $Ra_L=\frac{g\beta q_c L^4}{\rho\nu\alpha^2 c_p}$
- Aspect ratio $A=D/L$.

10.21611/qirt.2016.d

ONSET OF HORIZONAL CONVECTION

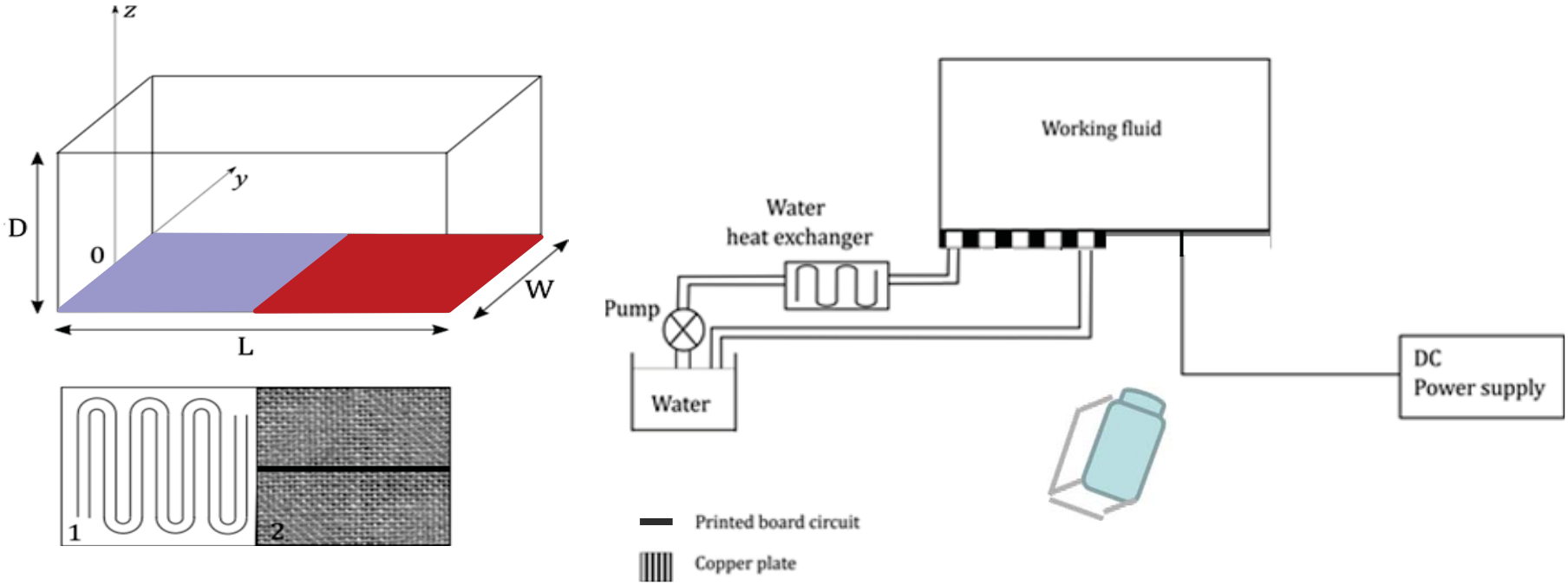

Schematic of the experimental apparatus

10.21611/qirt.2016.d

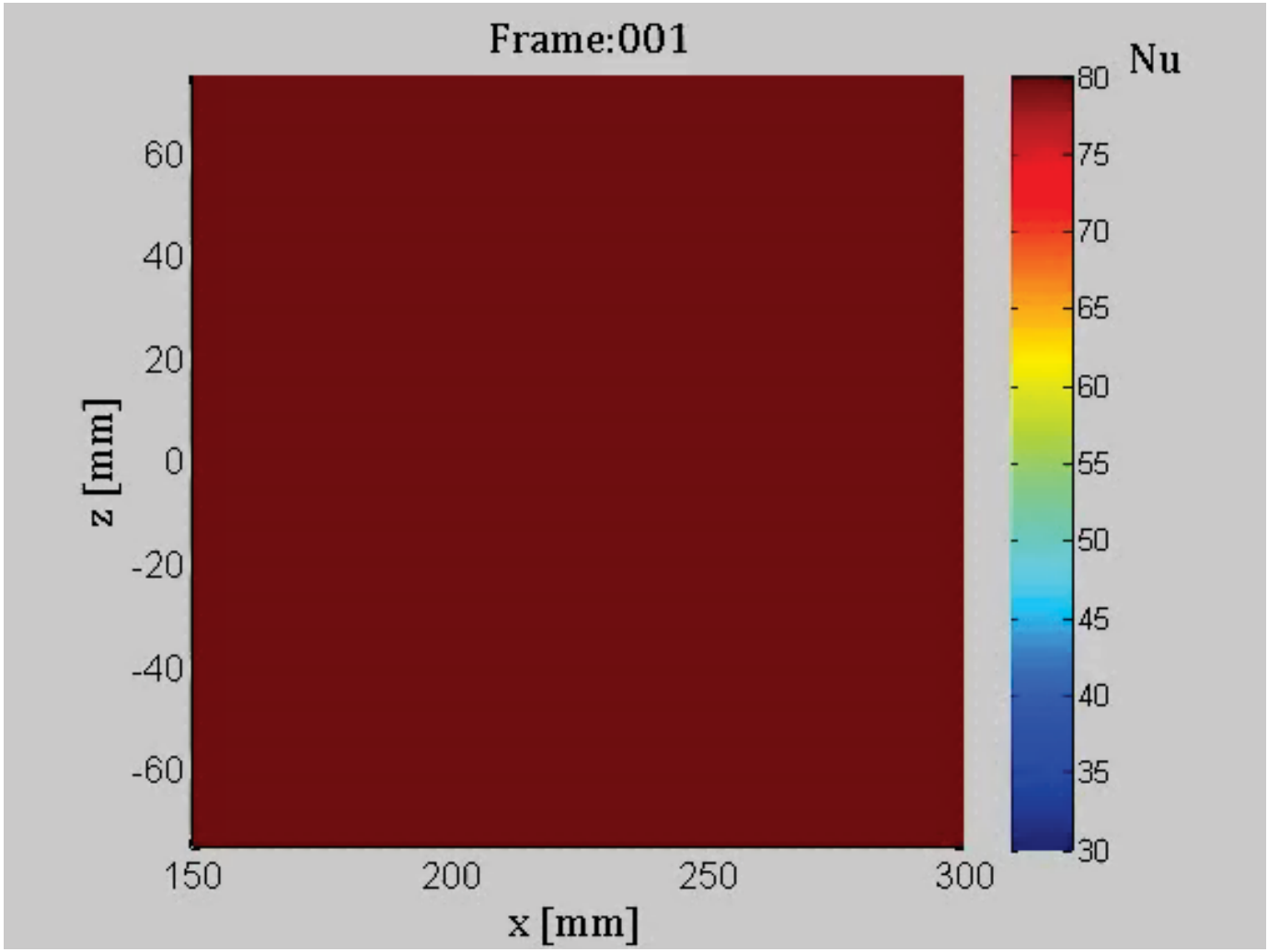

10.21611/qirt.2016.d

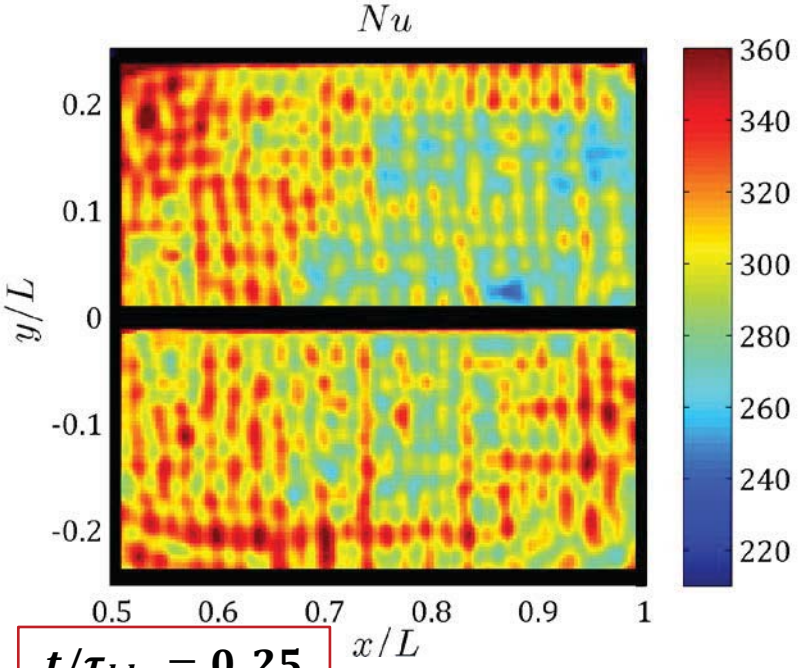

$t/\tau_{bl_0} = 0.25$

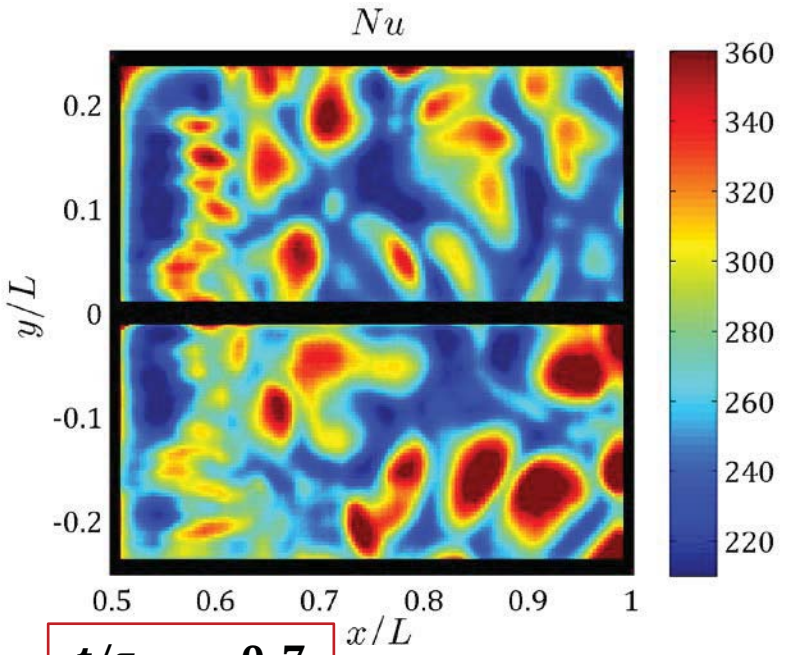

$t/\tau_{bl_0} = 0.7$

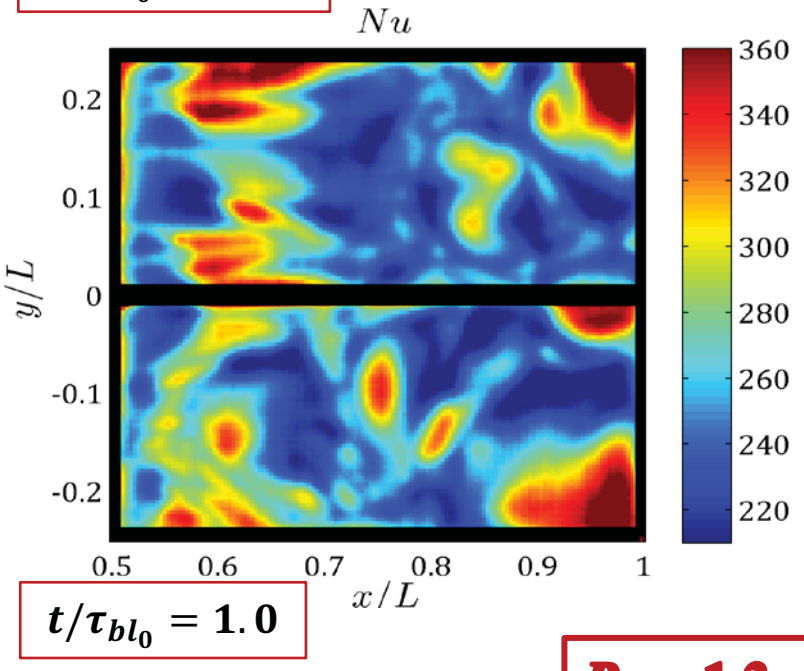

$t/\tau_{bl_0} = 1.0$

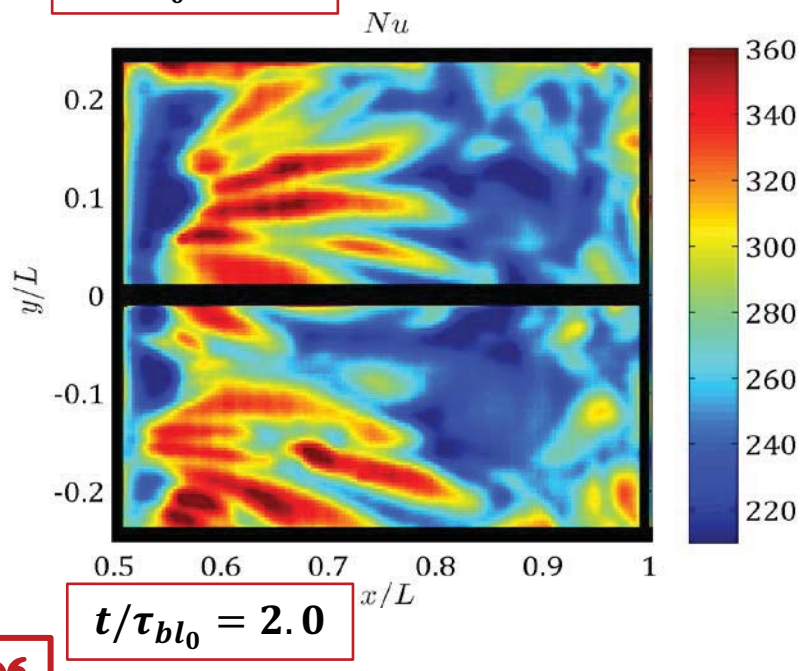

$t/\tau_{bl_0} = 2.0$

$Ra = 1.3 \times 10^6$

10.21611/qirt.2016.d

ELECTRONIC COOLING

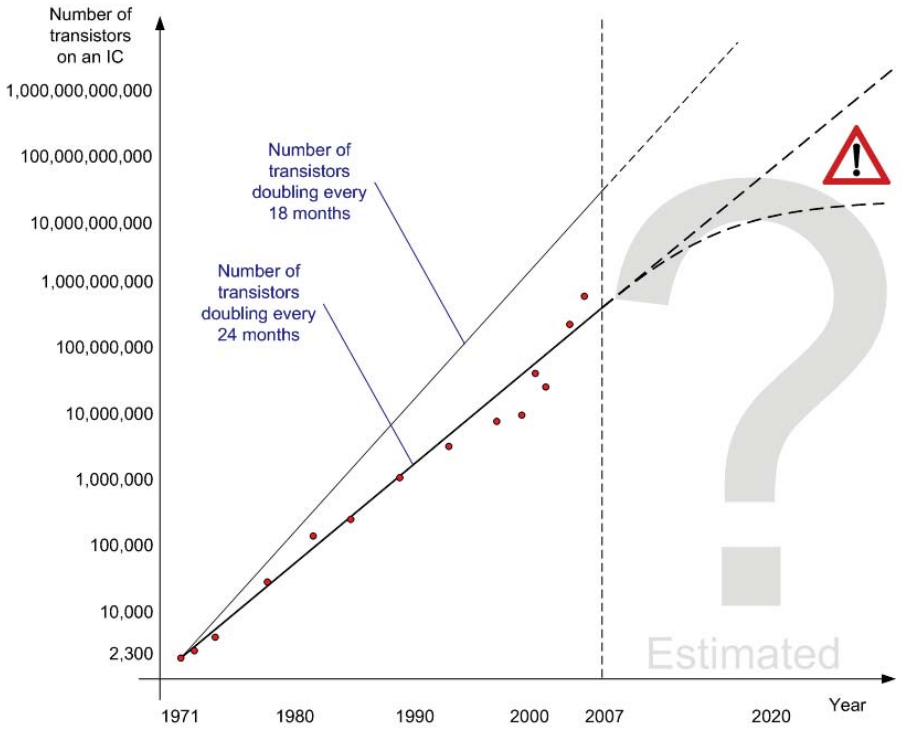

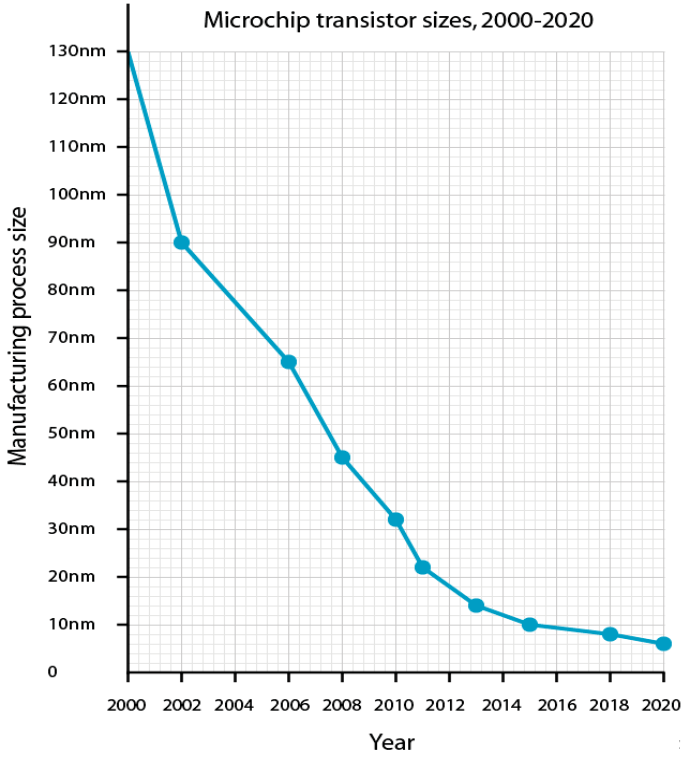

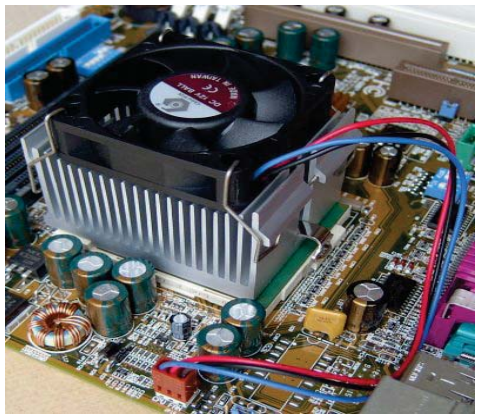

<u>Classical devices to cool:</u>

- Fan
- Heat Sink
- High conductivity materials

10.21611/qirt.2016.d

NEW PERSPECTIVES: SYNTHETIC JETS

- Zero net mass flow rate.
- Are generated by means of loudspeaker or a diaphragm movement in a cavity.
- Can be used in electronic cooling and flow control applications.

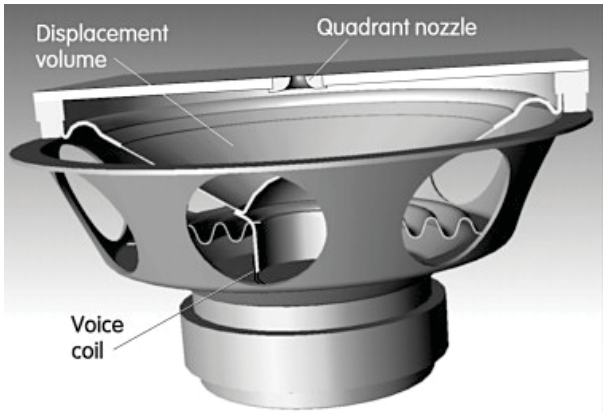

Loudspeaker

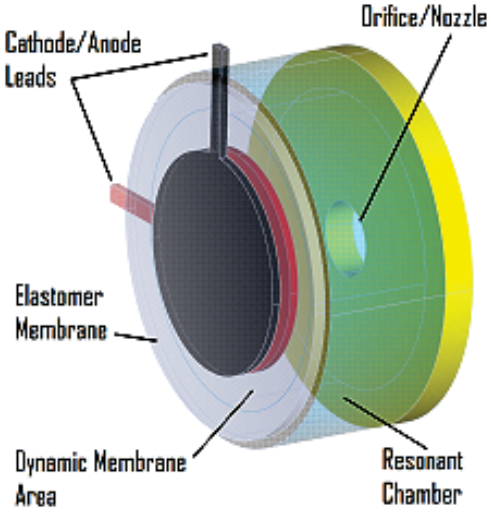

Piezoceramic

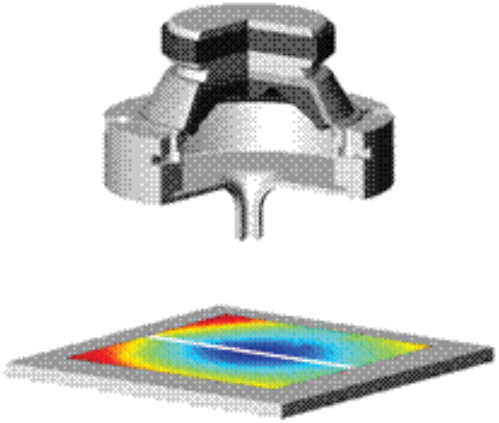

Impinging synthetic jet
(Murray D. B.)

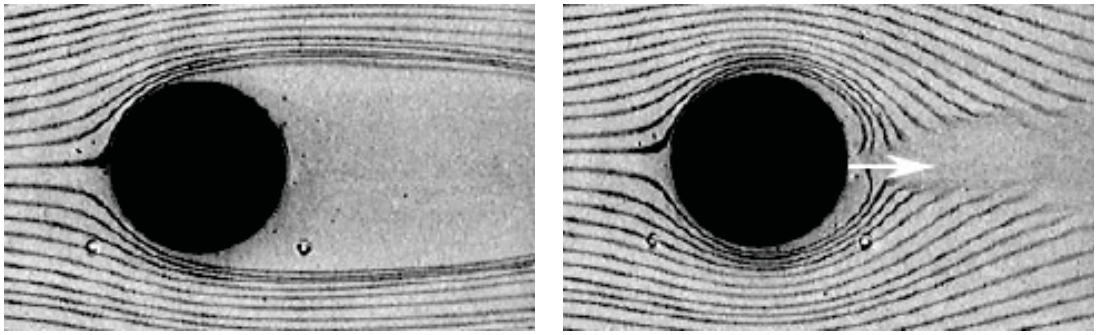

Flow control (Amitay M, et al., 1997)

De Luca L, Girfoglio M and Coppola G, Modeling and experimental validation of the frequency response of synthetic jets actuators, *AIAA J* (2014), 1-16

10.21611/qirt.2016.d

SYNTHETIC JETS (FLUID DYNAMICS)

Therefore, synthetic jets are produced by the interactions of a train of vortices that are typically formed by alternating momentary ejection and suction of fluid across an orifice (Glezer A, Amitay M, Synthetic jets, *Annu. Rev. Fluid Mech,* **34** (2002) 503-529).

The formation criterion for synthetic jets is:

$$\frac{Re}{S^2} > K$$

where K is a number whose value is 1 and 0,16 for plane two-dimensional and axisymmetric jets, respectively, Re the ***Reynolds number*** and S the ***Strouhal number*** ($S = V_m/2\pi f D$).

Holman R, Utturkar Y, Mittal R, Smith BL and Cattafesta L. Formation criterion for synthetic jets, *AIAA J,* **43** (2005) 2110-2116)

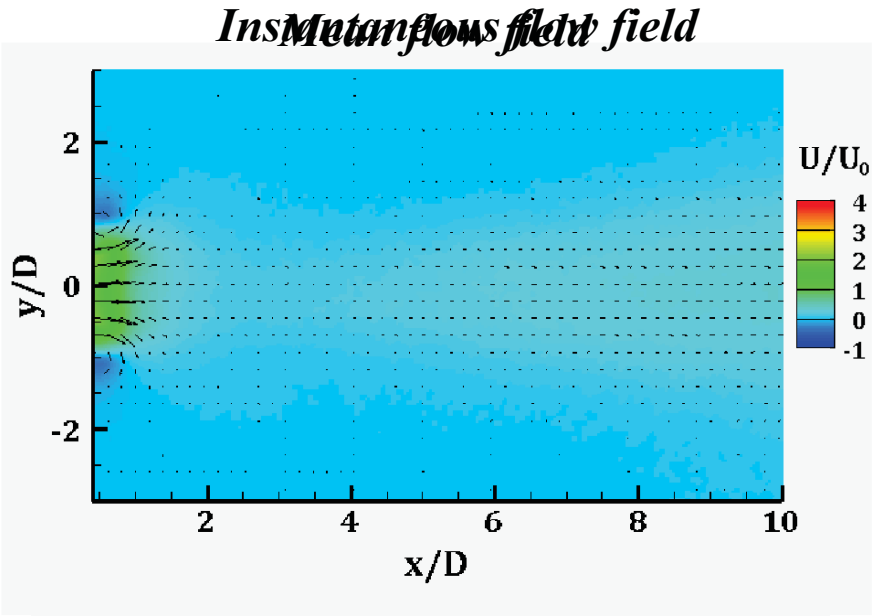

Phase averaged velocity

Greco CS, Ianiro A, Astarita T and Cardone G, On the near field of single and twin circular synthetic air jets, *acc. by Int. J. Heat Fluid Flow.*

10.21611/qirt.2016.d

SYNTHETIC JETS (HEAT TRANSFER)

The synthetic jet heat transfer is found to be comparable with the continuous axisymmetric jet and expected to be better at high Reynolds number. (Chaudhari M, Puranik B and Agrawal A, Heat transfer characteristics of synthetic jet impingment cooling, *Int. J. Heat Mass Transfer,* **53** (2010) 1057-1069)

Further understanding of the heat transfer mechanisms could be achieved exploiting time-resolved heat flux measurements, which is the objective of ongoing research.

(Valiorgue P, Persoons T, McGuinn A and Murray DB, Heat transfer mechanisms in an impinging synthetic jet for small jet-to-surface spacing, *Exp. Therm Fluid Sci*, **33** (2009) 597-603)

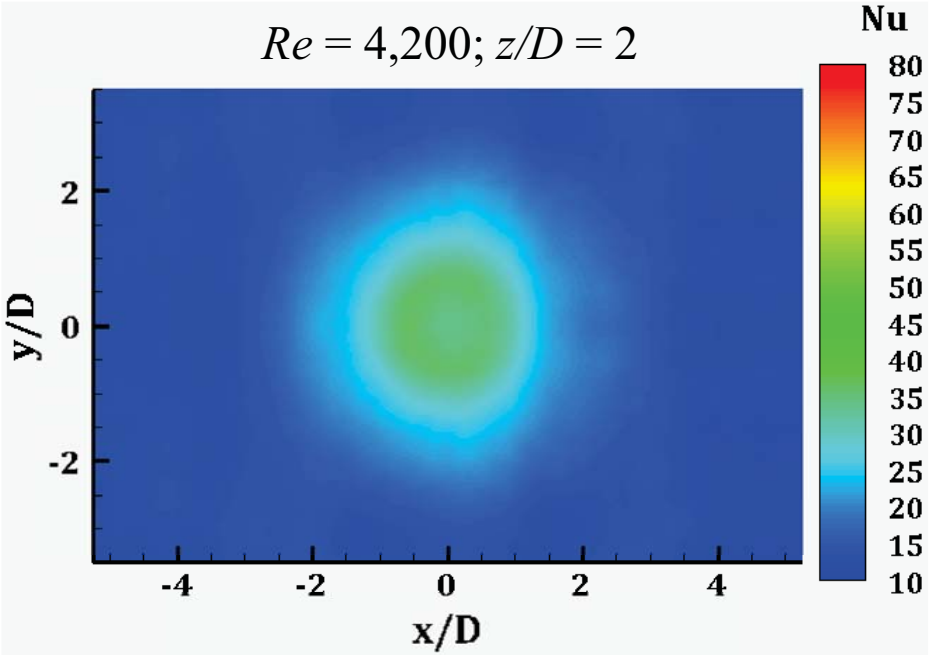

Phase averaged Nusselt number

Greco CS, Ianiro A and Cardone G, Time and phase average heat transfer in single and twin circular synthetic impinging air jets, *Int. J. Heat Mass Transfer,* 73 (2014) 776–788.

10.21611/qirt.2016.d

METHODS FOR HEAT TRANSFER ENHANCEMENT

- Acoustic excitation (Liu & Sullivan 1996);
- Application of swirl (Ianiro & Cardone 2012);
- **Introduction of mesh screens within the nozzle** (in particular ***fractal grids***);
- Introduction of perforated plates between nozzle and target plane (Lee et al 2002).

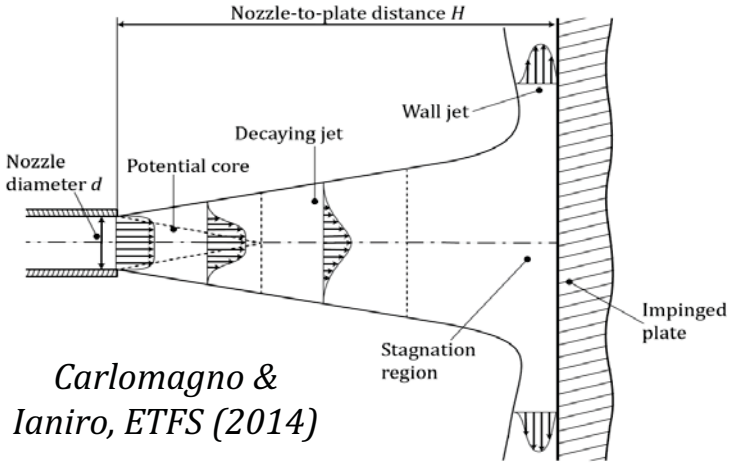

Carlomagno & Ianiro, ETFS (2014)

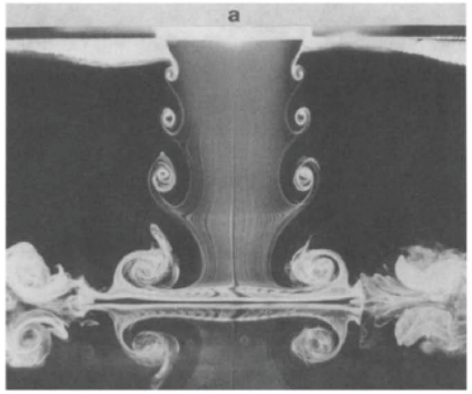

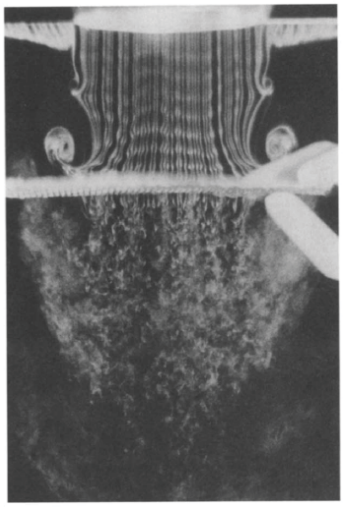

Popiel, ETFS (1991)

El Hassan et al, POF (2013)

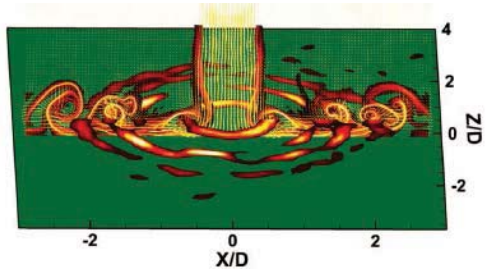

Violato et al, IJHFF (2012)

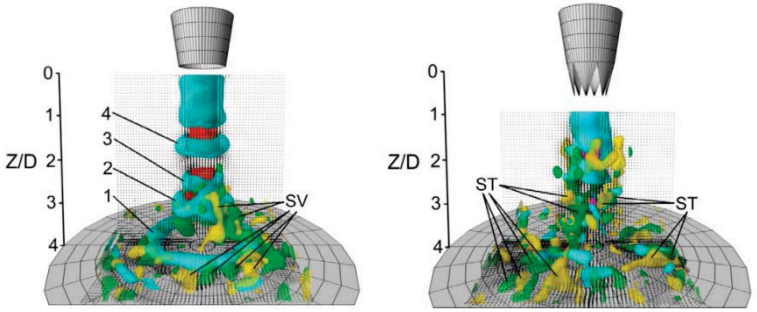

10.21611/qirt.2016.d

HOW TO OBTAIN A FRACTAL GRID?

Repeat the same pattern several time by scaling its dimensions

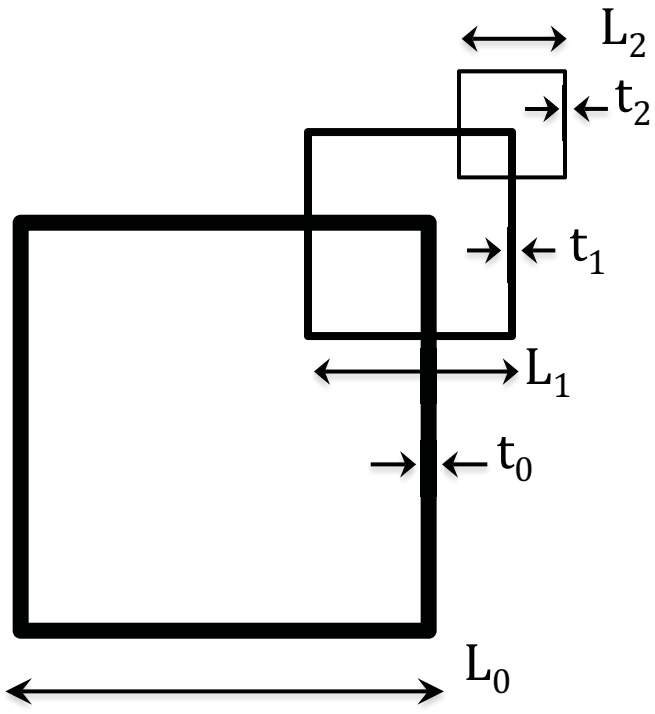

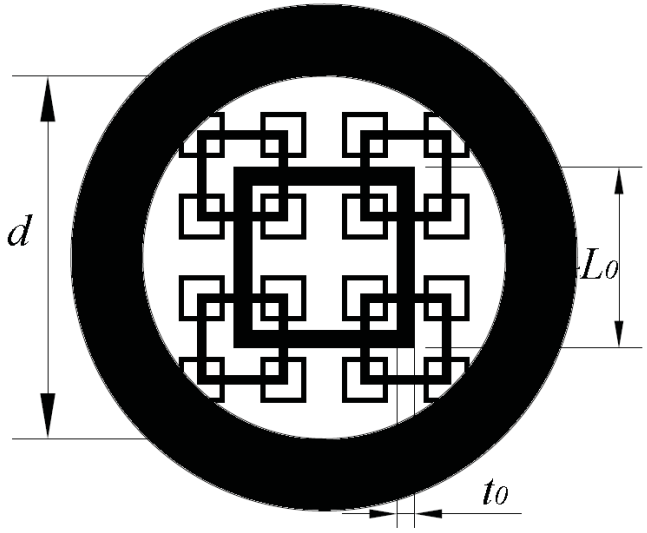

ACTUAL FRACTAL GRID	
L_0	10mm
t_0	1mm
L_r	4
t_r	4

10.21611/qirt.2016.d

EXPERIMENTAL SETUP

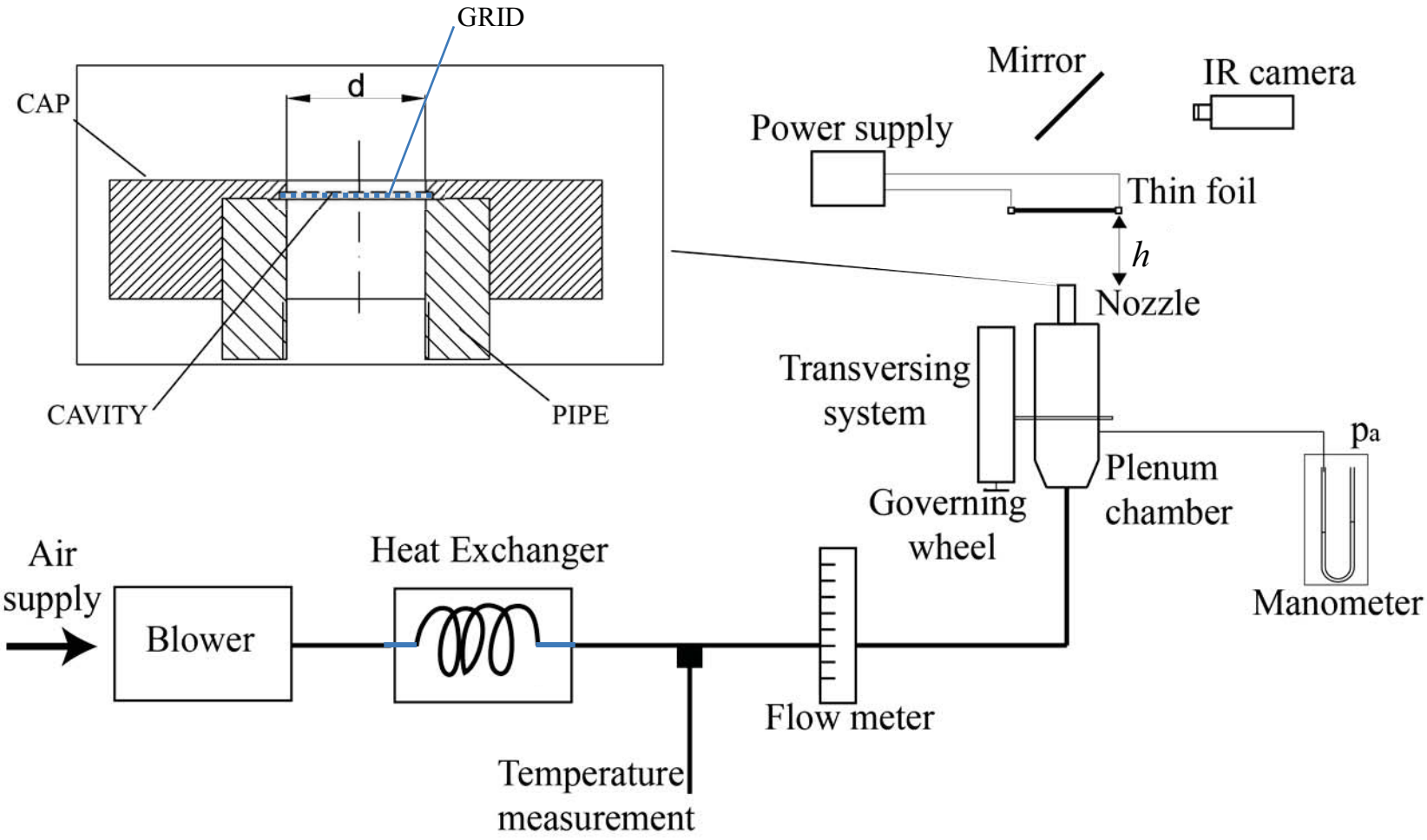

Infrared camera FLIR SC6000 ($640x512\ pixels, 3.2 pixels/mm$).

10.21611/qirt.2016.d

EXPERIMENTAL DETAILS

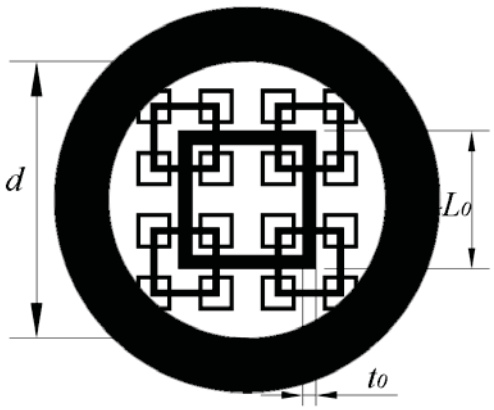

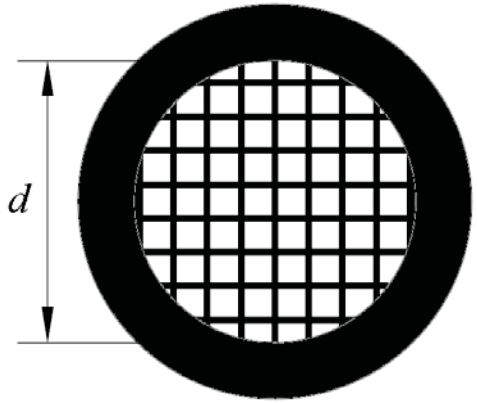

FRACTAL GRID	
L_0	10mm
t_0	1mm

REGULAR GRID	
M	2.4mm
b	0.4mm

Effective meshlength

$$M = \frac{\pi d^2}{P}\sqrt{1-\sigma}$$

Grid solidity

$$\sigma = \frac{b}{M}\left(2 - \frac{b}{M}\right) = 0.32$$

from Hurst & Vassilicos, POF (2007)

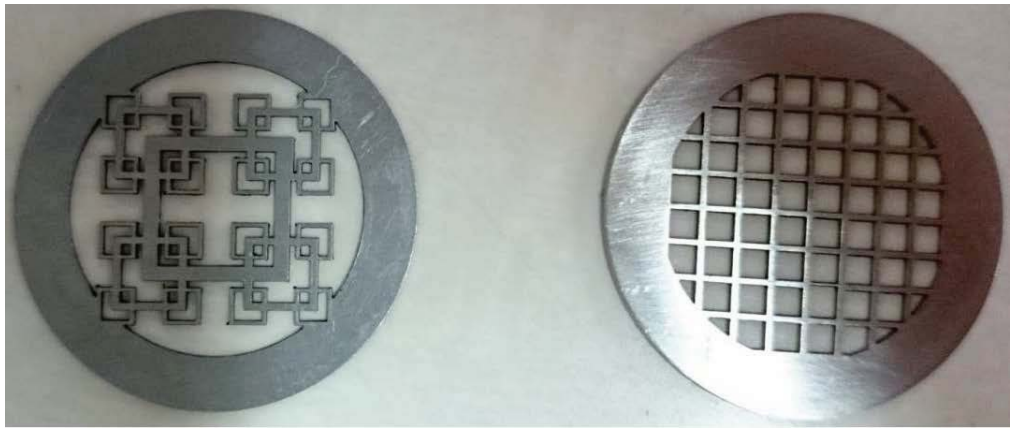

JWT **J**et **W**ithout **T**urbulators

RG **R**egular **G**rid

FG **F**ractal **G**rid

10.21611/qirt.2016.d

NUSSELT NUMBER DISTRIBUTIONS

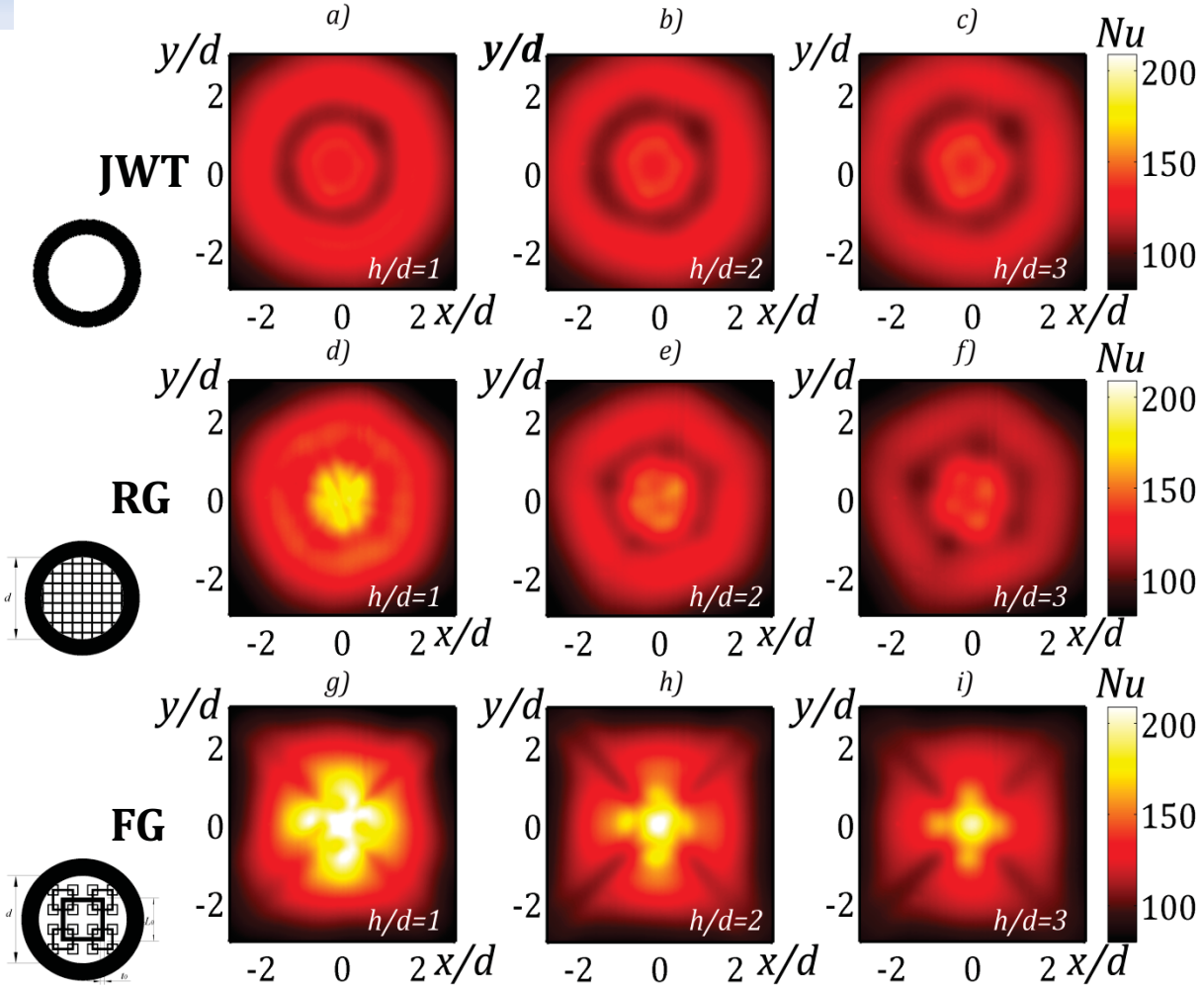

$$Re = 28,700$$

- Double peak due to ring vortices;
  Stagnation point heat transfer decreases as the distance increases.
- Multi-channel behaviour, with several local maxima in the *Nu* distribution.
- Strong HT enhancement in the stagnation region.
  Cross-shaped Nu map.

10.21611/qirt.2016.d

CONCLUDING REMARKS

Infrared Thermography represents an innovative methodology for ***heat transfer studies***, that we can use to either perform ***non-destructive testing*** as well as to ***measure convective heat fluxes***, its mean features being:

- provides a full ***two-dimensional*** information
- is a ***non-contact*** technique
- allows a ***computerized elaboration of the images***

The presented results were concerned with some significant experiments carried out during the past several years by the research group the presenter belongs to.

Through these results, it is proved that ***infrared thermography*** is able to yield ***valuable information*** about:

- ***non-destructive evaluation of materials***, markedly composites,
- accurate ***heat transfer measurements*** in complex fluid flows, especially if coupled with PIV.